Assessing the Adsorption Potential of Magnesium-Iron Layered Double Hydroxide Supported on Orange Peel (Mg-Fe LDH@OPP) for the Removal of Hexavalent Chromium from Wastewater

By

Waleed Usmani

Registration No. 00000328852

Supervisor

Dr. Muhammad Ali Inam

A thesis submitted in partial fulfillment of the requirements for the degree of Master of Science in Environmental Engineering

Institute of Environmental Sciences and Engineering,

School of Civil and Environmental Engineering,

National University of Sciences and Technology

Islamabad, Pakistan

(2023)

APPROVAL CERTIFICATE

Certified that the contents and forms of the thesis entitled.

"Assessing the Adsorption Potential of Magnesium-Iron Layered Double Hydroxide Supported on Orange Peel (Mg-Fe LDH@OPP) for the Removal of Hexavalent Chromium from Wastewater"

Submitted by

Mr. Waleed Usmani

Has been found satisfactory for partial fulfillment of the requirements of the degree of Master of Science in Environmental Engineering.

Dr. Muhammad Ali Inam
Assistant Professor
IESE (SCEE) NUST Islamabad

Supervisor: _____

Dr. Muhammad Ali Inam

Assistant Professor

SCEE (IESE), NUST

Dr. M. Bilal Khan Niazi
Professor, PhD
Chemical Engineering
SCME, NUST, Islamabad

GEC Member: _____

Dr. Muhammad Bilal Khan Niazi

Professor

SCME, NUST

Dr. Rashid Iftikhar
Assistant Professor
IESE (SCEE) NUST Islamabad

GEC Member: _____

Dr. Rashid Iftikhar

Assistant Professor

SCEE (IESE), NUST

ACCEPTANCE CERTIFICATE

It is certified that the contents and forms of the thesis entitled **"Assessing the Adsorption Potential of Magnesium-Iron Layered Double Hydroxide Supported on Orange Peel (Mg-Fe LDH@OPP) for the Removal of Hexavalent Chromium from Wastewater"** submitted by Mr. Waleed Usmani, Registration No. 00000328852 found complete in all respects as per NUST Regulations, is free of plagiarism, and mistakes and is accepted as partial fulfilments for award of MS degree. It is further certified that necessary modifications as pointed out by GEC members of the scholar have been included in the said thesis.

Dr. Muhammad Ali Inam
Assistant Professor
IESE (SCEE) NUST Islamabad

Supervisor: _____ 21/09/2023

Dr. Muhammad Ali Inam

SCEE (IESE), NUST

Dr. Zeshan
Tenured Assoc Prof
HoD Environmental Sciences
IESE (SCEE) NUST Islamabad

Head of Department: _____

Dated: 25/09/2023

Prof. Dr. Imran Hashmi
Associate Dean
IESE (SCEE) NUST Islamabad

Associate Dean: _____

Dated: 25-09-2023

PROF DR MUHAMMAD IRFAN
Principal & Dean
SCEE, NUST

Principal & Dean SCEE: _____

Dated: 25 SEP 2023

DECLARATION

I certify that this research work titled **"Assessing the Adsorption Potential of Magnesium-Iron Layered Double Hydroxide Supported on Orange Peel (Mg-Fe LDH@OPP) for the Removal of Hexavalent Chromium from Wastewater"** is my own work. This work has not been presented elsewhere for evaluation. The material that has been used from other sources has been properly acknowledged.

Waleed Usmani

00000328852

PLAGIARISM CERTIFICATE

I certify that this research work titled "Assessing the Adsorption Potential of Magnesium-Iron Layered Double Hydroxide Supported on Orange Peel (Mg-Fe LDH@OPP) for the Removal of Hexavalent Chromium from Wastewater" is my own work. Thesis has significant new work as compared to already published or under consideration to be published elsewhere. The thesis has been checked using TURNITIN and found within limits as per HEC plagiarism Policy and instructions issued from time to time.

Signature of Student:_____

Dr. Muhammad Ali Inam
Assistant Professor
IESE (SCEE) NUST Islamabad

Signature of Supervisor:_____ 21/09/2023

DEDICATION

This endeavor would not have been possible without the support of my exceptional parents, adored sibling, and my friends whose tremendous support and cooperation led me to this wonderful accomplishment.

"By virtue of whose prayers, we have been able to attain this position and whose hands are always raised for prayers, for our well-being."

ACKNOWLEDGEMENT

First and foremost, I acknowledge that it is by the grace of Allah Almighty that I have been able to complete this manuscript. All respect to the Holy Prophet (P.B.U.H) whose life is the model I am trying to base my life around.

Next, I express my utmost thanks to my supervisor Dr. Muhammad Ali Inam, who has supported and guided me throughout my research. His keen interest and valuable suggestions have helped me overcome all obstacles encountered during my research work. I will forever be thankful for his incredible guidance, encouragement, and sympathetic attitude during the entire period of my research.

This acknowledgement would be incomplete if I didn't pay my sincere and hearted thanks to my cherished and loving parents and sister for their sacrifices, prayers, and affections without which it would have been nearly impossible to achieve my goals. The belief my friends exhibited in me pushed me towards the finish line. I would also thank other institutes for their continuous support and encouragement throughout my time at NUST. Last but not least I would like to thank all the laboratory staff at IESE for their help and cooperation.

Waleed Usmani

TABLE OF CONTENTS

LIST OF FIGURES

LIST OF TABLES

ABSTRACT

Herein, a series of meticulously designed batch and continuous mode sorption experiments were conducted to compare removal affinity of raw orange peel powder (OPP) and magnesium-iron layered double hydroxide impregnated OPP (Mg-Fe LDH@OPP) composite for the elimination of Cr (VI) ions from aqueous media. The relatively greater particle size, irregular pore distribution, effective surface area, and higher point of zero charge (pH_{pzc}) of Mg-Fe LDH@OPP as compared to OPP were principally responsible for its superior Cr (VI) sorption from aqueous media. It was observed that highest Cr (VI) removal (OPP: 81.84%; Mg-Fe LDH@OPP: 100%), was achieved at optimum conditions of pH (2), adsorbent dosage (2 g/L), contact time (180 min) and temperature (25°C) for suspension containing 20 mg/L initial Cr (VI) concentration. The sorption data was adequately fitted with Freundlich and pseudo-second order model using both biosorbents. The FT-IR and XRD analysis further confirmed the reduction pathway followed by complexation reactions as major sorption mechanisms using Mg-Fe LDH@OPP. However, in the case of OPP, ligand exchange played a critical role in removing Cr (VI) ions from water. Furthermore, continuous mode column studies suggested applicability of Mg-Fe LDH@OPP compared to raw OPP. The results indicated breakthrough times of up to 366 min and 60 min, and exhaustion times of up to 800 min and 350 min, for Mg-Fe LDH@OPP and OPP, respectively. In general, Mg-Fe LDH@OPP was found to be a promising material with strong Cr (VI) sorption potential from polluted water.

CHAPTER 1

INTRODUCTION

1.1. Background

Environmental pollution is the biggest and most serious leading problem in recent times. With the rapid growth in population, there has been an increase in industrialization, use of fossil fuels and increased consumption of natural and synthetic resources, which is leading to major environmental hazards in a lot of countries, including Pakistan. These environmental hazards include air pollution, soil pollution and water contamination. Particularly, the increased rate of industrialization is considered to be one of the leading causes of water pollution.

Water is considered to be the most essential resource to sustain life and the environment we live in. However, in today's age, a major crisis of water has been observed and it is reported that over eight billion humans are being affected by it, according to WWF. Pakistan is also facing major water crisis where only 930 m3 water per capita is accessible annually. Urban development, increasing industrialization along with increase in irrigation needs for the purpose of agriculture are known to be the major factors contributing to the depletion of quality and quantity of country's water resources, resulting in reduced agricultural output, ultimately impacting the health of the population.

Toxic metals like arsenic (Carneiro et al., 2022), lead (Wahid et al., 2021), antimony (Inam et al., 2021) and chromium (Moges et al., 2022) poses adverse effects on human life and environment, making their pollution a worldwide issue. Because of their non-decomposable characteristic, they cause substantial environmental risks. Researchers from across the world are working to eliminate or significantly lower the levels of these heavy metals in wastewater.

The contamination of water bodies with chromium (Cr) species has received significant attention globally owing to its toxicological and carcinogenic risks to humans (Barrera-Díaz et al., 2012; Li et al., 2017; Miretzky & Cirelli, 2010). It occurs in multiple oxidation forms, including trivalent Cr (III) under reducing environment, and hexavalent Cr (VI) in aerobic conditions (Barnhart, 1997). Various natural and anthropogenic activities may be responsible for high Cr (VI) concentration in natural water bodies. For instance, post release of untreated Cr laden wastewater from steel and metal processing industries, electroplating and leather tanning processes may present elevated Cr (VI) concentration in water bodies globally (GracePavithra et al., 2019). Considering such scenario, highly Cr (VI) contaminated sites are evident in the industrial regions of Pakistan, with exceeding safe levels from 6,900 to 19,500 mg/kg in soil and from 19.90 to 13.53 mg/L in drinking water reservoirs (Chandio et al., 2021). Such an alarming Cr (VI) concentration may cause human health issues including lung cancer, skin irritation, rashes, ulceration, allergic reactions, respiratory problems, and genetic mutations etc. (Sharma et al., 2022). Therefore, for the protection human health, World Health Organization (WHO) and Pakistan Environmental Protection Agency (Pak-EPA) has set maximum permissible level of 0.05 mg/L Cr species in drinking water.

1.2. Introduction to Chromium

In the periodic table's group 6, Chromium is the first element with Cr as its symbol and 24 as its atomic number. In addition, one can easily find it in rocks, volcanic dust, soil and gases (Saha et al., 2022). Trivalent chromium is the most naturally occurring form of chromium and is denoted by Cr (III). It is a non-toxic form and is mainly available in food and supplements. The less common occurring form of chromium is hexavalent chromium, denoted by Cr (VI). It is found in industrial runoff and is toxic and carcinogenic when inhaled or consumed orally (Hayashi et al., 2021). Even at low quantities, exposure to chromium can be dangerous, and its removal is still a difficult problem for researchers in the present era.

1.3. Application of Chromium

Chromium, as a metal, has a wide usage in industries due to its unique properties. Stainless steel production is achieved by the usage of Chromium, which is a highly corrosion resistant material. It is added to steel to form a thin, hard, protective layer to avoid the rusting of an underlying metal (Yu et al., 2018). It is often used in electroplating to provide a hard, durable, and corrosion resistant coating to various metal surfaces, including automobile trim and household appliances (Danilov et al., 2006). Chromium is also used to produce soft and durable leather products, such as clothing and upholstery through the process of leather tanning (Sreeram & Ramasami, 2003). Another use of chromium is in various industrial processes, such as the production of nitric acid, organic chemicals, and synthetic fibers, where it is used as a catalyst (MacAdams et al., 2005). It is used in the production of pigments and dyes, including chrome green and chrome yellow, which are used several applications, including paint and ink (Verger et al., 2018). As an alloying element, it is used in the production of high strength alloys, such as tool steels, which are used in several applications, including the aerospace and automotive industries (Gerard et al., 2023).

1.4. Sources of Chromium

As it is so commonly used in industries, chromium can be released into the environment in the form of wastewater, air emissions and solid waste. Chromium containing waste, such as chrome plated metal and leather tanning waste can end up in landfills where it can leach into the soil and groundwater, contaminating these resources. Also, accidents and spills during the transport and storage of chromium containing products can release the substance into the environment, potentially contaminating nearby water sources and soil. Furthermore, chromium containing minerals in rocks and soils can also weather and release chromium into the environment, contaminating water and soil. Once released into the environment, chromium can persist for a long time and can travel long distances, making it difficult to clean up and control.

1.5. Exposure to Chromium

It can enter the body through a number of ways. It can be inhaled as dust or fumes during industrial processes or while working with chromium containing products. Inhaling chromium can lead to the substance entering the bloodstream and potentially causing health problems. Prolonged skin contact with chromium containing products, such as chrome plated metal or leather treated with chromium, can cause the substance to be absorbed into the skin and enter the

bloodstream. Chromium can enter the body when it is consumed in food, drinking water, or through the use of dietary supplements. The amount of chromium absorbed through oral intake varies depending on the type and form of chromium and the individual's health and diet. It can also enter the body through injection, such as in the case of medical treatments that involve the use of chromium containing compounds. Once in the body, chromium can be distributed to various tissues and organs, where it can potentially cause health problems, depending on the type of chromium, the level of exposure and the duration of exposure.

1.6. Effects of Chromium

Being exposed to chromium can have adverse effects on one's health. If one's skin is exposed to Cr (VI) he can suffer from lung cancer, as well as skin irritation, rashes, ulceration, and allergic reactions (Wang et al., 2017). Inhaling Cr (VI) dust or fumes can cause respiratory problems, such as bronchitis, lung irritation, and shortness of breath (S. Adachi, 1987). Cr (VI) has also been found to damage DNA and cause genetic mutations, which can increase the risk of cancer and other health problems (Bianchi et al., 1983). Some people can develop an allergic reaction to Cr (VI), which can cause skin itching, redness and swelling (Bregnbak et al., 2015). Moreover, high levels of chromium exposure can cause kidney and liver damage, as well as other health problems.

1.7. Problem Statement

The quality of groundwater has been adversely impacted because of population growth and industrial expansion. The environment and the public health of millions of people all over the world are potentially at risk due to the contaminated groundwater caused by the presence of chromium metal from the tanning and leather industry. The chromium metal exists as Chromium (III) and Chromium (VI) in natural environment. Chromium (VI) is a known carcinogen that can harm the lungs, irritate the skin, and even lead to cancer.

Pakistan produces large number of citrus fruits per annum. According to a recent study, in 2021, Pakistan produced 2.33 million tons of citrus fruit, growing at an average annual rate of 3.95%. The peel of citrus fruit is discarded, increasing waste generation, which already is a huge problem in thickly populated areas of Pakistan. Orange peel is considered as a good adsorbent material because of its properties like high surface area and porous structure, which makes it effective at capturing and retaining impurities and contaminants from water. Furthermore, the compounds present in orange peel like phenols and flavonoids are known for their adsorption properties. In the present study, orange peel was utilized as an adsorbent and was further activated by magnesium, iron and layered double hydroxide for the removal of chromium from aqueous media.

1.8. Research Objectives

Moving further, the objectives of this research work are stated as:

- Comparison of the surface properties of bimetallic layered double hydroxide functionalized orange peel composite with its raw form.
- Examination of the effect of water chemistry parameters on the sorption behavior of Cr (VI) ions using batch and continuous mode experiments.
- Examination of the mechanistic insights into the sorption behavior of Cr (VI) ions from aqueous matrices using characterization tools.

CHAPTER 2

LITERATURE REVIEW

2.1. Cr (VI) Removal Technologies

Several treatment techniques including coagulation (T. Xu et al., 2019), membrane separation (Mondal & Saha, 2018), electrochemical processes (H. Peng et al., 2019) and bioremediation (Ayele & Godeto, 2021) have been previously applied to eliminate heavy metals, including Cr (VI) from water. However, high capital and operating cost, greater sludge generation and microbial toxicity limit their applications for subsequent use at large scale operations (Karimi-Maleh et al., 2021). Therefore, exploring indigenous and low-cost sorbents for treatment of targeted Cr (VI) species may present cost effective and efficient solution to drinking water industry. To date, researchers have examined various raw biosorbents i.e., sweet lime peel (Shakya et al., 2019), moringa leaves (Madhuranthakam et al., 2021), potato peel (Mutongo et al., 2014), peach and apricot stones (Pertile et al., 2021) and orange peel (JishaTJ et al., 2017) for their effectiveness towards Cr (VI) species from water. Amongst, many researchers have explored the effectiveness of raw orange peel for removing pollutants including arsenic (Irem et al., 2017), selenium (Dev et al., 2020), ammonia (Dey et al., 2021), nitrate (Dey et al., 2021), copper (Feng et al., 2010), cadmium (Akinhanmi et al., 2020) and antimony (Hasan et al., 2021) from water. However, raw orange peel presented regeneration and stability issues along with high sludge volume production. Therefore, it will be critical to explore surface functionalization approaches of orange peel for further enhancing the removal of Cr (VI) ions from water.

There are numerous methods for chromium removal. Typical methods for removing chromium include:

- Chemical precipitation
- Coagulation-flocculation
- Electrocoagulation
- Ion exchange
- Membrane filtration
- Adsorption

2.1.1. Chemical Precipitation

The type of separation method where contaminating ions are pushed out of the solution by chemical precipitants, allowing for physical separation to remove them is known as chemical precipitation. During this process, pollutants settle as precipitates, which are then filtered, centrifuged, or removed using other suitable techniques. A coagulant act as a precipitating agent which causes the suspension of small particles in a solution which then enlarges and settles as sludge. Chemical precipitators that are frequently used as coagulant include sodium hydroxide, calcium hydroxide, magnesium oxide, and calcium magnesium carbonate. Researchers have

utilized this method for the removal of Cr (VI) ions using sodium metabisulphite ($Na_2S_2O_5$) (Basavaraju & Ramakrishnaiah, 2012) and sodium hydroxide (NaOH), calcium hydroxide ($Ca(OH)_2$) and magnesium oxide (MgO) (Chandravanshi & Leta, 2017) as reducing agents with removal efficiencies of 99.7% and 99.97%, 99.97% and 99.98%, respectively. Chemical precipitation is an extremely simple, cost-effective, and highly efficient process. It is a pH and temperature sensitive process and does have some limitations including high sludge generation and regular maintenance and monitoring.

2.1.2. Coagulation-Flocculation

The coagulation-flocculation method is frequently utilized in the treatment of water and wastewater due to its efficiency in eliminating suspended particles and other contaminants. Chemical coagulants are added to the targeted wastewater to facilitate the flocculation of small particles into large particles. These particles are then allowed to settle down and are separated using various separation techniques. This process is widely used to separate organic substances, suspended particles, and heavy metals like chromium. Chromium contamination in wastewater can decrease the efficacy of biological treatment, like that found in municipal wastewater treatment facilities. Hence, this technique is used as a first stage method to reduce the overall load of chromium. This method has been utilized in research for the removal of Cr (VI) using ferric chloride and organic polymer(Amuda et al., 2006) and polymeric ferric sulphate(D. Xu et al., 2019) as coagulants with Cr (VI) removal efficiency of 91%, 95% and 98.3%, respectively. This process is, however, time consuming and does generate a lot of sludge which requires proper disposal or further treatment, which ultimately increases the overall cost and complexity of the treatment process.

2.1.3. Electrocoagulation

Electrocoagulation is an electrochemical water and wastewater treatment process that uses direct current to destabilize and remove suspended particles, colloids, and other contaminants and heavy metals like chromium from water. It is a modification of the conventional coagulation process that makes use of metal ions produced by electrochemical processes rather than just chemical coagulants. In this procedure, electrodes composed of sacrificial metals, such as iron, aluminum, or other reactive materials, are used. These electrodes are placed in the targeted wastewater, and electrochemical reactions occur at their surface when a direct current is provided. This process leads to the dissolution of metal and the release of metal ions into the water. These metal ions function as coagulants, neutralizing the charges on colloids and suspended particles to encourage floc formation. Then, through the use of settling, flotation and other filtration techniques, these flocs are removed from the water. Different research has been conducted to remove Cr (VI) using electrocoagulation with iron (Genawi et al., 2020) and titanium (G. J. Li et al., 2019) electrodes with Cr (VI) removal efficiency of 100% and 91%, respectively. It is a highly energy efficient process with minimum sludge generation. However, it is costly, pH sensitive and requires electrode maintenance.

2.1.4. Ion Exchange

Ion exchange is a method of treating water that involves the exchange or removal of ions from a solution using a solid substance namely as ion exchange resin. This method is widely employed in many different applications, such as water softening, demineralization, deionization, water purification, and wastewater treatment. The ion exchange resin is a polymer containing charged functional groups that may draw and bind ions with opposing charges. Since the resin often comes in the form of tiny beads or granules, there is a lot of surface area available for ion exchange to occur.

The two most popular forms of ion exchange resins are known as cation exchange resins and anion exchange resins. Functional groups with a negative charge, like sulfonate or carboxylate groups, are present in cation exchange resins. These functional groups draw and exchange the solution's positively charged ions. Calcium (Ca^{2+}), magnesium (Mg^{2+}), sodium (Na^{+}), and potassium (K^{+}) are examples of common cations that can be exchanged. On the other hand, anion exchange resins contain functional groups that are positively charged, such as quaternary ammonium or amine groups. The negatively charged ions in the solution are drawn to and exchanged by these groups. Chloride (Cl^{-}), sulfate (SO_4^{2-}), nitrate (NO_3^{-}), and carbonate (CO_3^{2-}) are typical anions that can be exchanged.

During the ion exchange procedure, the solution is passed through an ion exchange resin column or bed. The ions in the solution are exchanged with the ions coupled to the functional groups on the resin as the solution and resin come into contact with each other. The original ions are released into the treated solution as the exchanged ions are attached to the resin. Researchers have used alkaline anion resin(AHMAD et al., 2020) and Amberlite 252 ZU cation exchange resin (Kocaoba et al., 2022) for the removal of Cr (VI) from wastewater with removal efficiency of 98% and 95%, respectively. While ion exchange is a versatile and effective water treatment process, it does have some disadvantages and limitations like competing ions including phosphate, sulphate and carbonate that reduce removal efficiency, high cost, regeneration of resin and waste disposal.

2.1.5. Membrane Filtration

Membrane filtration is a separation technique that clears water of impurities by using semi-permeable membranes. It is a physical separation technique that divides materials according to the size exclusion principle by running the targeted liquid stream across a semi-permeable filtration membrane. The membrane has precisely crafted pores that permit the passage of the liquid stream and smaller particles while trapping the desired contaminants. It is an efficient and frequently used technique for treating water that has been contaminated with chromium compounds. Some of the membrane filtration techniques frequently used for chromium separation include ultrafiltration (Korus & Loska, 2009), nanofiltration (Zolfaghari & Kargar, 2019), reverse osmosis (Çimen, 2015), and electrodialysis (C. S. L. Dos Santos et al., 2019). Sometimes different kinds of membrane filtration are used one after another to prolong the life and improve performance of the membranes while still removing adequate chromium.

2.1.6. Adsorption

The adhering process of atoms, ions, or molecules from a gas, liquid, or solution to the surface of a solid material is known as adsorption. This phenomenon occurs due to attractive forces between the surface of the solid and the particles of the gas or liquid. The effectiveness of adsorption is due to various aspects which include the properties of the adsorbent material, the nature of the adsorbate, temperature, pressure, and surface area available for adsorption. Several adsorbents have been studied and shown promising results for the removal of Cr (VI) from water and wastewater. The effectiveness of an adsorbent can vary based on factors such as its surface area, porosity, surface chemistry, and cost. It's important to note that the effectiveness of Cr (VI) removal through adsorption can be influenced by various factors, such as the initial concentration of Cr (VI), temperature, adsorbent dosage, and the presence of other competing ions in the solution. Therefore, optimization of these parameters is essential to achieve efficient and economical chromium removal from water sources. Some of the most effective adsorbents for Cr (VI) removal are as under:

2.1.6.1. Activated Carbon

Activated carbon is an excellent adsorbent for the removal of Cr (VI) from water and wastewater due to its high surface area, porosity, and strong affinity. However, it is essential to manage the spent activated carbon properly, as it will contain the adsorbed Cr (VI) and may need to be disposed of or treated safely to prevent further contamination. Additionally, combining activated carbon adsorption with other treatment processes, like reduction or precipitation, can further enhance Cr (VI) removal efficiency and ensure comprehensive water treatment. Activated carbon prepared from mango kernel was used in research (Rai et al., 2016) to remove Cr (VI) from wastewater. The maximum adsorption capacity was calculated as 7.8 mg/g at 2 pH and temperature of 35 °C.

2.1.6.2. Iron Oxide Based Adsorbents

Iron oxide-based adsorbents are known to be effective for the removal of Cr (VI) from water due to their strong affinity for chromium ions. These adsorbents generally consist of iron oxide minerals, such as magnetite (Fe_3O_4) or hematite (Fe_2O_3), which have high surface area and surface reactivity. Overall, iron oxide-based adsorbents are attractive for Cr(VI) removal due to their availability, cost-effectiveness, and potential for both adsorption and reduction processes. The following research (Park et al., 2022)a chitosan-coated iron oxide nanoparticle immobilized hydrophilic poly(vinylidene)fluoride membrane (Chi@Fe2O3–PVDF) was used as adsorbent to remove Cr (VI) ions from wastewater, achieving high adsorption capacity of 14.451 mg/g in batch system and 14.104 mg/g in continuous flow system.

2.1.6.3. Zeolites

Zeolites are crystalline aluminosilicate minerals with a unique structure characterized by regular and uniform pore sizes. Due to their porous nature and ion-exchange properties, zeolites have shown significant potential for the removal of various pollutants, including Cr (VI), from water and wastewater. Zeolites have cation exchange sites on their surface, which can attract, and exchange cations present in the surrounding solution. In the case of Cr (VI) removal, divalent or trivalent cations (e.g., Na^+, K^+, Ca^{2+}) present in the zeolite structure can exchange

with Cr (VI) anions ($HCrO_4^-$ and CrO_4^{2-}), leading to Cr (VI) adsorption on the zeolite surface. Research was conducted by using natural zeolite and zeolite synthetized with NaOH activation to remove Cr (VI) from industrial wastewater. It was determined that the highest Cr (VI) removal for both natural and synthetized zeolite was 82% and 56%, respectively.

2.1.6.4. Agricultural Byproducts

The removal of Cr (VI) from adsorbents obtained from agricultural byproducts is an effective and sustainable approach for wastewater treatment. Agricultural byproducts often contain natural materials with porous structures and functional groups that can serve as adsorption sites for Cr (VI) ions. This method not only helps in reducing environmental pollution but also makes use of renewable resources, contributing to waste valorization and sustainability. Certain agricultural waste byproducts, such as rice husk ash, sawdust, and sugarcane bagasse, can be modified to serve as low-cost adsorbents for Cr (VI) removal. Researchers have used oat waste (Gardea-Torresdey et al., 2000), sawdust of beech (Acar & Malkoc, 2004), modified rice husk bagasse (Bishnoi et al., 2004) and neem leaf powder (Özer et al., 1994) to remove Cr (VI) ions from wastewater and achieved removal efficiency of 80%, 100%, 89% and 96%, respectively.

2.1.6.5. Modified Agricultural Biproducts

Previously, modification of biosorbents with phosphoric acid (Enniya et al., 2018), sulfuric and nitric acids (Prajapati et al., 2020) and zinc chloride (Kumar & Jena, 2017), have also shown strong potential in the sorption of Cr (VI) anions from aqueous medium. In addition, orange peel impregnated with calcium alginate, sodium hydroxide, acetic acid, and calcium hydroxide, respectively, have been used to remediate selenium (Dev et al., 2020), copper (Feng et al., 2010), antimony (Hasan et al., 2021) and arsenic (Y. Peng et al., 2013) from aqueous solutions.

2.1.6.6. Layered Double Hydroxides

In the current state, layered double hydroxide (LDH) has garnered considerable interest in current years due to its numerous applications in catalysis, adsorption, nanotechnology, and biotechnology (Kang et al., 2013). In laboratory and industrial scales, they are simple and affordable to produce (Elmoubarki et al., 2017). The layered structure, broad chemical composition, varied layer charge density, ionic exchange characteristics, active space between layers, expansion in water, rheometric, and nanocrystalline capabilities make LDH a clay-mineral like substance (Forano et al., 2013). In lieu, previous research (Meili et al., 2019) presented maximum sorption capacity (406.47 mg/g) for methylene blue using magnesium-aluminum LDH (Mg-Al LDH) composite. Yet, exposure to Al for long periods of time has been identified as a possible concern factor for the ecosystem as well as human health. Considering this, it is vital to look for new materials devoid of harmful metals. In this regard, iron (Fe) based LDH compounds have also shown promising performance in the elimination of hazardous anions from water (Kang et al., 2013). For instance, Mg-Fe LDH has been applied in conjunction with chloride (L. C. Santos et al., 2020) and with nanoscale hydroxyapatite (Guo et al., 2020) to remove nitrate and uranium, respectively. Similarly, various studies (Maamoun, Bensaida, et al., 2022; Maamoun, Falyouna, et al., 2022)indicate 100% Cr (VI) removal using magnesium

hydroxide-coated iron nanoparticles and nickel hydroxide nanoplates from contaminated suspensions. Another study (Eljamal et al., 2022)presented good sorption affinity (22.1 mg/g) of Mg-Al-LDH towards boron from aqueous solution.

Therefore, investigating the removal capacity of Mg-Fe LDH in combination with orange peel powder for the removal of Cr (VI) ions from water would also be significant. To date, no research has been done to remediate Cr (VI) ions from water using Mg-Fe LDH modified orange peel composite.

CHAPTER 3

METHOD AND MATERIALS

3.1. Material

Orange peels were taken from a local market in Lahore, Punjab, Pakistan. These said peels were washed with distilled water, allowed sun-drying for 4 days, followed by oven drying at 40℃ for about one hour (Hasan et al., 2021). Afterwards, the dried orange peels were grinded to powder form, sieved through a mesh 10 (2 mm) sieve and stored in air-tight packs. The orange peel powder (OPP) was then kept in sealed desiccators before use.

3.2. Chemicals

The reagent grade chemicals such as iron (III) chloride hexahydrate ($FeCl_3.6H_2O$), magnesium chloride hexahydrate ($MgCl_2.6H_2O$), potassium dichromate ($K_2Cr_2O_7$) and 1,5-diphenylcarbazide were obtained from Sigma Aldrich (USA). Other chemicals including sodium hydroxide (NaOH), hydrochloric acid (HCl), potassium dihydrogen phosphate (KH_2PO_4), potassium nitrate (KNO_3), sodium sulphate (Na_2SO_4), sodium chloride (NaCl), sodium bicarbonate ($NaHCO_3$) and acetone were purchased from local vendors.

3.3. Preparation of Stock Solution

The 1000 mg/L Cr (VI) stock solution was prepared by dissolving 0.285 g $K_2Cr_2O_7$ in 100 mL distilled water. The working solutions of desired Cr (VI) concentration were then prepared by spiking the required volume of stock solution in distilled water, as per experimental conditions. Moreover, 0.1 M HCl and 0.1 M NaOH solutions were prepared to adjust the solution pH. In addition, all glassware and sampling vessels were washed with 15% HNO_3 solution, followed by rinsing with distilled water prior to adsorption experiments.

3.4. Synthesis of Mg-Fe LDH@OPP

The co-precipitation method was employed for the preparation of magnesium-iron layered double hydroxide supported on orange peel powder (Mg-Fe LDH@OPP). In brief, 10 g OPP was added in a suspension containing 0.03 M $MgCl_2$ and 0.01 M $FeCl_3$. Afterwards, suspension pH was set to 10 using 0.1 M NaOH solution. The obtained slurry was kept in an oven at 70°C for 3 days to eliminate all moisture and was then thoroughly grinded to obtain powder form Mg-Fe LDH@OPP (Xue et al., 2016). Prior to experimental use, the obtained composite was cleaned with distilled water, overnight dried in an oven at 100°C and then stored in air-tight packs in desiccators.

3.5. Experimental Conditions and Procedure

A series of batch experiments were conducted using 20 mg/L Cr (VI) suspensions to assess the removal capabilities of OPP and Mg-Fe LDH@OPP. Initially, the influence of adsorbent dosages (0.1, 0.2, 0.5, 1, 2, 3 and 5 g/L) was investigated at pH 2 and contact time of 120 min. The sorption performance of both adsorbents was also evaluated at varying pH conditions (2, 3, 4, 5, 6, 7, 8 and 9) using sorbent dosage (2 g/L) and contact time (120 min). The kinetic study of OPP and Mg-Fe LDH@OPP was carried out by allowing both adsorbents to

react with Cr (VI) solutions at different time intervals (0, 30, 45, 60, 90, 120, 180 and 240 min) at pH 2 and adsorbent dosage (2 g/L). Afterwards, further experiments were conducted using biosorbent dosage (2 g/L) at pH 2 and contact time (180 min). The isotherm study was then performed by allowing both sorbents to react with varying concentration of Cr (VI) suspensions (1, 2, 5, 10, 15, 20, 30, 50, 75 and 100 mg/L). Furthermore, thermodynamic investigations of OPP and Mg-Fe LDH@OPP were conducted at varying solution temperatures of 25, 35 and 45°C for Cr (VI) suspensions of 50 mg/L. The regeneration potential of OPP and Mg-Fe LDH@OPP was also evaluated over 5 adsorption cycles for Cr (VI) suspensions of 20 mg/L. Moreover, the influence of coexisting anions such as PO_4^{3-}, NO_3^-, SO_4^{2-}, Cl^- and HCO_3^- on Cr (VI) removal was investigated under varying pH conditions (2, 4 and 6) in 20 mg/L Cr (VI) suspensions. Furthermore, the point of zero charge (pH_{pzc}) of both adsorbents was calculated at varying pH conditions of 2, 3, 4, 5, 6, 7, 8 and 9. All experiments were conducted in duplicates and average values with relative standard deviations were reported.

An orbital shaker was utilized for performing adsorption studies at 200 rpm mixing speed. However, a shaking incubator (Korea) was used to conduct experiments at controlled temperature conditions and at mixing speed of 120 rpm during thermodynamic studies. After post-sorption experiments, all samples were filtered using 0.22µm GE cellulose nylon membrane filter. A reagent was prepared by adding 0.5 g of 1,5-diphenylcarbazide into 100 mL of acetone (Rattanarat et al., 2013). 2 mL of this reagent was added into the filtrate along with 3 to 4 drops of phosphoric acid (H_3PO_4). The filtrate was then analyzed using spectrophotometric method. A UV-Vis spectrophotometer (SPECORD 200, Analytikjena, Germany) was used to examine the filtrate at 540 nm wavelength.

3.6. Calibration Curve

Solutions having different Cr (VI) concentrations of 0.1, 0.2, 0.5, 1, 1.5 and 2 mg/L were used to prepare the calibration curve. The R^2 value of the curve was 0.999. The data of the calibration curve is given in **Table 1** and **Figure 1** below:

Table 1: Cr (VI) calibration curve

Concentration (mg/L)	0.0	0.1	0.2	0.5	1.0	1.5	2.0
Absorbance	0.0000	0.0997	0.2246	0.4630	0.8744	1.2793	1.6792

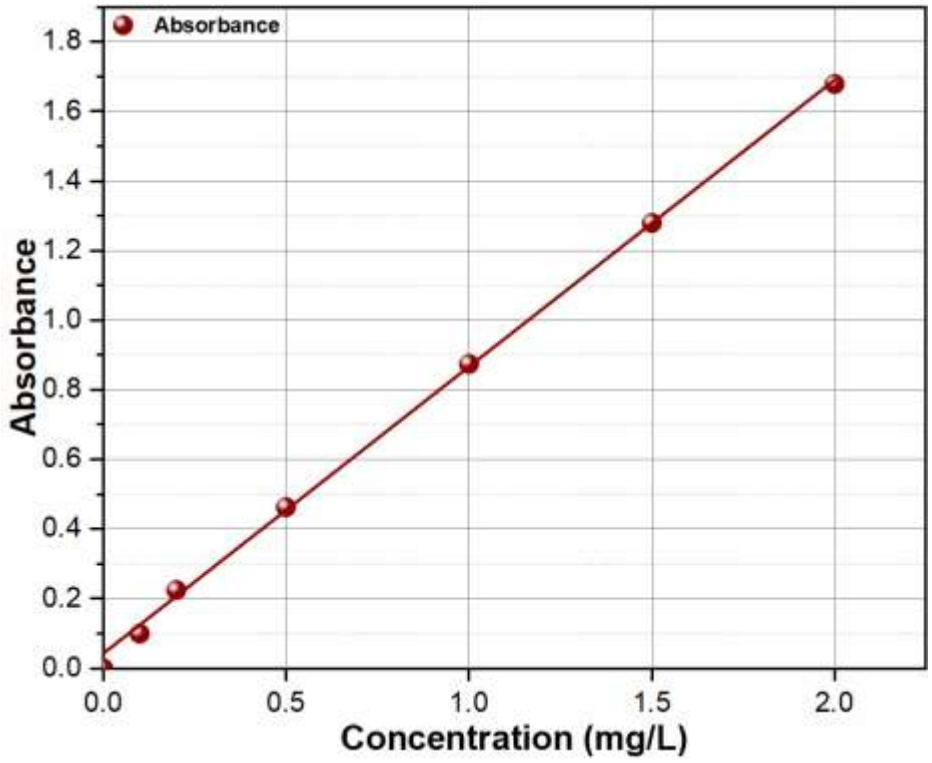

Figure 1: Cr (VI) calibration curve

3.7. Final Concentration and Adsorption Capacity

The residual chromium concentration was calculated using the following Eq. (1) and Eq. (2):

Adsorption capacity: $q_e = \frac{(C_o - C_e)V}{m}$ **(1)**

Removal efficiency: $R = \frac{(C_o - C_e)}{C_o} * 100\ \%$ **(2)**

Where C_e and $C_o$are the residual and initial Cr (VI) concentrations (mg/L) in the solutions, m is the mass of biosorbent (g), and V is the initial volume of suspension (L).

3.8. Kinetic Models

For the investigation of the kinetics of the adsorbent, non-linear forms of the Lagergren pseudo-first order (PFO) and pseudo-second order (PSO) equations were used which are mentioned as Eq. (3) and Eq. (4) below:

PFO equation: $q_t = q_e - e^{\ln(q_e) - k_1 t}$ **(3)**

PSO equation: $q_t = \frac{k_2 q_e{}^2 t}{1 + k_2 q_e t}$ **(4)**

Where the contact time is expressed in t (min), q_e (mg/g) is the adsorption capacity of the adsorbent at equilibrium, q_t(mg/g) is the adsorption capacity of the adsorbent at different time intervals, $k_1$is the PFO rate constant and $k_2$is the PSO rate constant.

3.9. Isotherm Models

For the study of isotherms of the adsorbent, Eq. (5) and Eq. (6) were used which are mentioned below:

Langmuir equation: $q_e = \frac{q_m k_L C_e}{1+k_L C_e}$ **(5)**

Freundlich equation: $q_e = k_F C_e^{\frac{1}{n}}$ **(6)**

Where q_e (mg/g) is the adsorption capacity of the adsorbent at equilibrium, C_e (mg/L) is the final chromium concentration, q_m (mg/g) is the maximum adsorption capacity of the adsorbent, k_L (L/mg) is Langmuir constant related to adsorption energy, k_F $[(g/mol)(L/mg)]^{1/n}$is a constant related to the adsorption capacity, and n is an index of heterogeneity.

3.10. Thermodynamic Studies

For the determination of the thermodynamics parameters of the adsorbent, following Eq. (7), Eq. (8) and Eq. (9) were used:

Equilibrium constant: $k_c = \frac{q_e}{C_e}$ **(7)**

Gibbs free energy: $\Delta G = -RTlnk_c$ **(8)**

Thermodynamics parameters: $\Delta G = \Delta H - T\Delta S$ **(9)**

Where q_e (mg/g) is the adsorption capacity of the adsorbent at equilibrium, C_e (mg/L) is the final chromium concentration, R (8.314 J/mol.K) is the universal gas constant, T (K) is the absolute temperature, ΔH (intercept) is the enthalpy and ΔS (slope) is the entropy obtained by the linear fitting of ΔG versus T.

3.11. Fixed Bed Column Studies

The fixed bed column studies were conducted utilizing a polypropylene column with a 1.5 cm internal diameter, 12 cm length and adsorbent's bed depths of 0.5 and 1.0 cm, respectively. The ascending flow rate of 2 mL/min flow rate of Cr (VI) solution (20 mg/L) at pH 2 was pumped through column and remaining Cr (VI) concentration was monitored at various time intervals until remaining and initial Cr (VI) concentration become equal. To illustrate the column bed performance, a breakthrough curve was created from the plot of *P*/*Po* against time. The dynamic adsorption model i.e., Yoon-Nelson model was then employed on experimental data to explore breakthrough curve behaviors and variations under various bed depths. The Yoon-Nelson model is expressed as the following Eq. (10):

$$\frac{P}{Po} = \frac{1}{1 + e^{K_{YN(T-t)}}} \quad (\mathbf{10})$$

Where P and P_o are the residual and initial Cr (VI) concentrations (mg/L) in the solutions, T is the time required for 50% adsorbate breakthrough (min). K_{YN} is the Yoon-Nelson rate constant (min^{-1}), and t is the flow time (min).

3.12. Analytical Procedures

Scanning Electron Microscopy (SEM) (Japan) was used to obtain high resolution surface images of raw OPP and Mg-Fe LDH@OPP, which revealed its micro and nano scale morphologies. Similarly, energy dispersive X-ray spectroscopy (EDX) was used to examine the elemental composition of the biosorbents. Brunauer-Emmett-Teller (BET) was used to analyze the pore volume, pore radius and surface area of raw OPP and Mg-Fe LDH@OPP. The samples were dried at 105℃ for 24 hours to remove all moisture. A BET surface area analyzer (USA) was used to assess the adsorption isotherm at liquid nitrogen temperature (-196.15℃). Samples were degassed under vacuum conditions. Subsequently, using the P/P_o ratio, the BET surface area of both biosorbents was assessed. The bonding features and chemical composition of OPP and Mg-Fe LDH@OPP, before and after reaction with Cr (VI) were assessed using Fourier Transform Infrared Spectroscopy (FT-IR) (USA) between wavenumber of 400–4000 cm^{-1}. Moreover, X-ray diffraction (XRD) (Germany) was analyzed using Cu Kα radiations at 2θ from 0° to 90° to identify the variations in crystalline structure of raw and spent adsorbents. In addition, chemical equilibrium software Visual MINTEQ was used to obtain speciation diagram of Cr (VI) species. Moreover, the popular graphing software OriginPro 2018 was used to plot the experimental data.

3.13. Degree of Crystallinity and Crystallite Size

The degree of crystallinity (DOC%) was calculated using the following Equ. (11):

$$\text{DOC: } Xc = \frac{Ac}{Ac + Aa} \quad (\mathbf{11})$$

Where Ac is the area under crystalline diffraction patterns and Aa is the area under amorphous diffraction patterns. Similarly, the crystalline size was calculated using the following Equ. (12):

$$\text{Crystallite size: } D = \frac{K\lambda}{\beta \cos\theta B} \quad (\mathbf{12})$$

Where D, K, λ, β, and θ_B represent crystallite size (nm), shape constant (K = 0.9), X-ray wavelength (λ = 0.154 nm), peak width at half maximum height (radians), and reflection angle (radians), respectively.

CHAPTER 4

RESULTS AND DISCUSSION

4.1. Characterization of OPP and Mg-Fe LDH@OPP

4.1.1. Morphological Analysis

4.1.1.1. SEM of OPP

SEM images were used to examine the surface texture and topology of OPP and Mg-Fe LDH@OPP. As can be seen in **Figure 2**, OPP presented irregular and distinct surface characteristics with vertical and uneven distribution of pores within the surface.

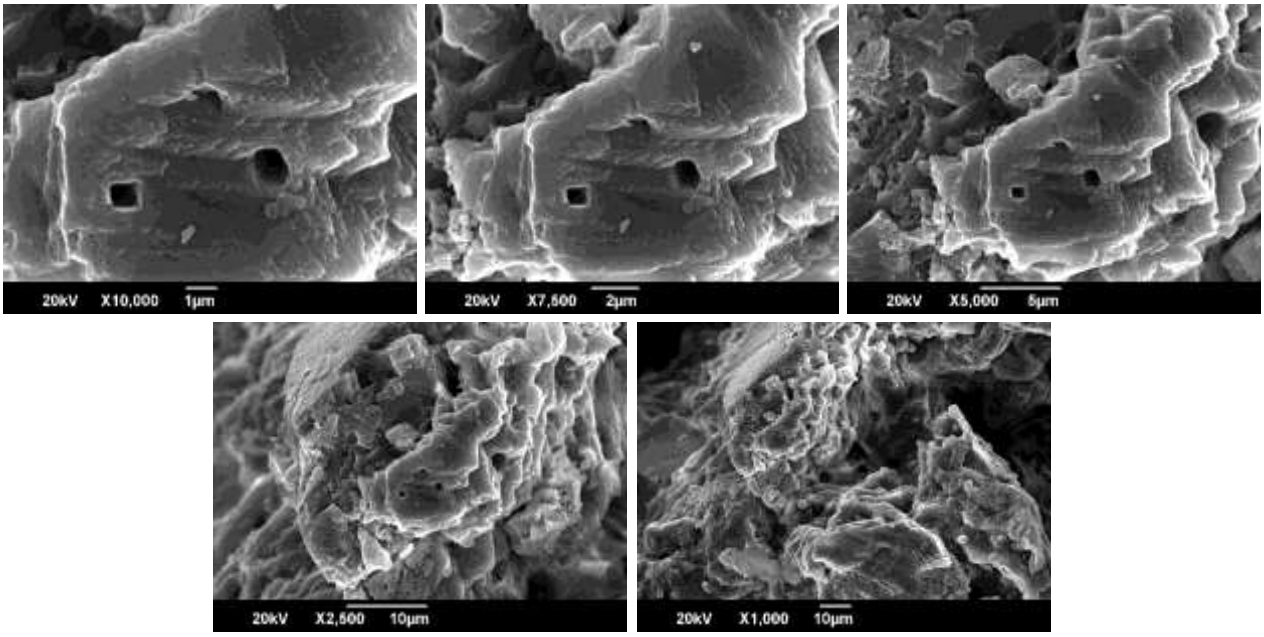

Figure 2: SEM images of OPP

4.1.1.2. SEM of Mg-Fe LDH@OPP

As seen in **Figure 3**, SEM images of Mg-Fe LDH@OPP showed an increase in the porosity and surface roughness. The small particle size and uneven particle distribution on the Mg-Fe LDH@OPP surface may also be responsible for increasing the effective surface area, which may provide better sorption potential than OPP towards contaminants from aqueous solutions. Similarly, changes in structural features in LDH based composite were also observed in previous study (Guo et al., 2020), which indicated uneven particle distribution in the original orderly layered structure owing to in-situ growth of LDH with nano scale hydroxyapatite.

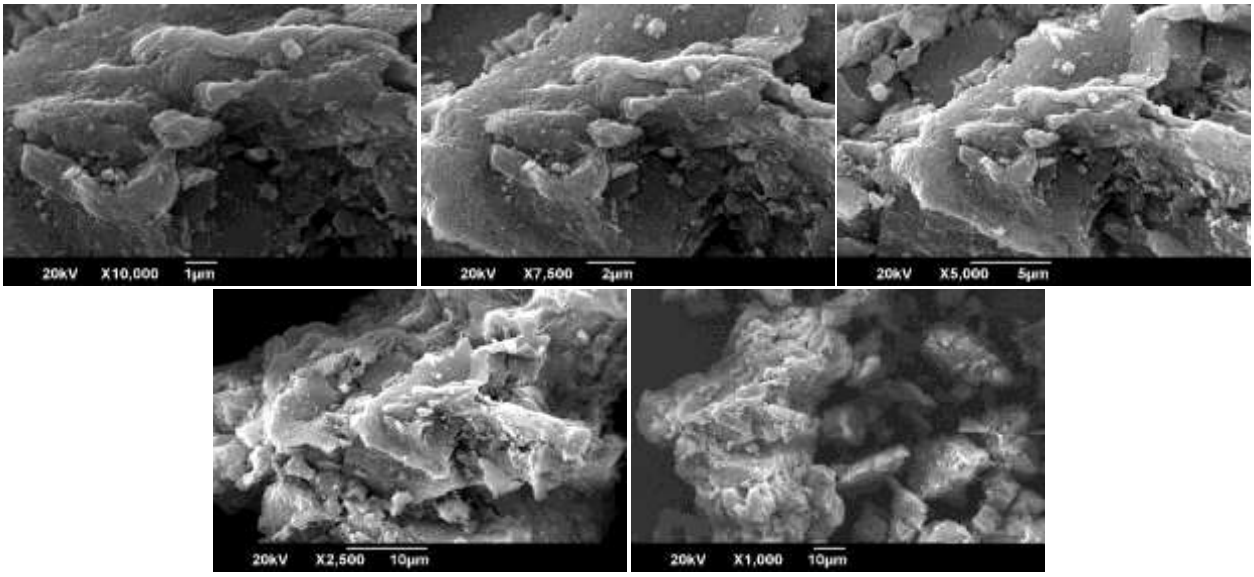

Figure 3: SEM images of Mg-Fe LDH@OPP

4.1.2. Elemental Composition Analysis

4.1.2.1. EDX of OPP

The EDX data of OPP and Mg-Fe LDH@OPP was also acquired to determine the chemical composition of different elements in both adsorbents. As shown in **Figure 4**, the three major peaks of C, O and Ca were detected in OPP with percentage distribution as 17.8%, 52.7% and 28.6%, respectively.

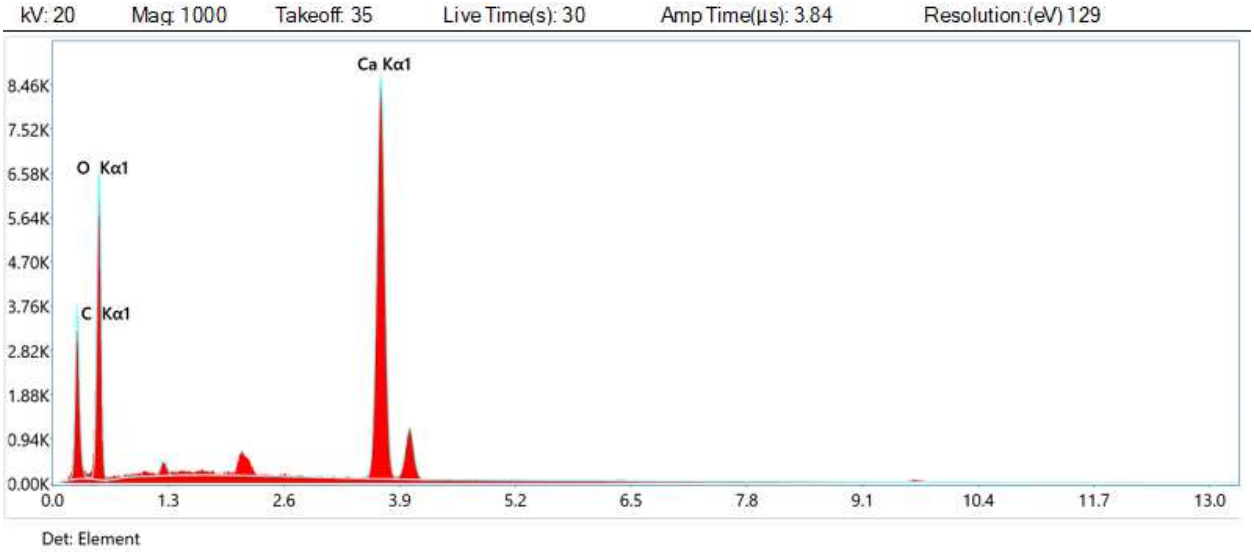

Figure 4: EDX of OPP

4.1.2.2. EDX of Mg-Fe LDH@OPP

After modification of OPP with Mg-Fe LDH, additional peaks of Fe and Mg with percentage distribution as 18.5% and 0.8% were also detected at selected surface site of modified adsorbent, as can be observed in **Figure 5**. In general, the results of SEM-EDX confirmed the

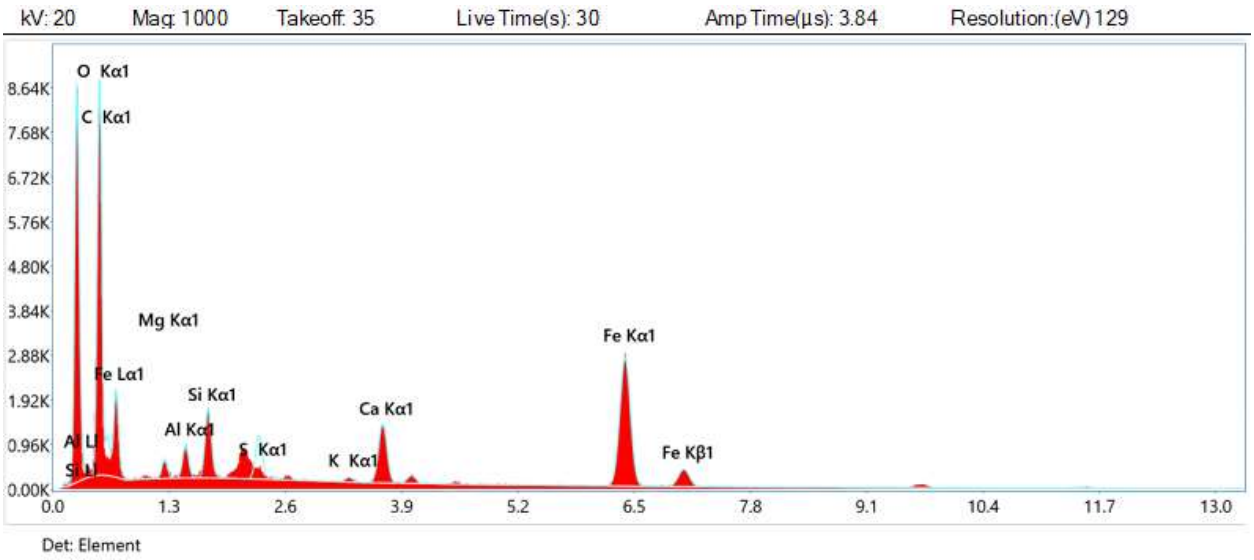

Figure 5: EDX of Mg-Fe LDH@OPP

formation of bimetallic layered double hydroxide in Mg-Fe LDH@OPP surface.

4.1.3. BET Analysis

BET analysis and Barrett-Joyner-Halenda (BJH) model were used to determine the microstructure characteristics of both adsorbents. As shown in **Table 2**, it was observed that the surface area of Mg-Fe LDH@OPP (18.810 m^2/g) was significantly greater than that of OPP (3.970 m^2/g). Similar trend was also observed in pore volume where it increased from 0.003 m^3/g to 0.008 m^3/g after modification of the adsorbent (Dey et al., 2021). The presence of magnesium and iron on the adsorbent's surface could be the reason behind the increase in the surface characteristics, which can eventually enhance its adsorption capacity.

Table 2:Textural property of OPP and Mg-Fe LDH@OPP

Adsorbent	Surface Area (m^2/g)	Pore Volume (m^3/g)	Pore Radius (nm)
OPP	3.97	0.003	1.607
Mg-Fe LDH@OPP	18.81	0.008	1.605

4.1.4. N_2 Adsorption/Desorption Isotherms

The liquid nitrogen (N_2) adsorption/desorption isotherms of OPP and Mg-Fe LDH@OPP are shown in **Figure 6(a, b)**. The results indicated that N_2 desorption didn't follow same pattern as that of adsorption with steep increase in volume of both adsorption and desorption isotherms. The characteristic hysteresis loop was formed which indicated that during adsorption, the process

of pore filling was due to capillary condensation, whereas during desorption, the process of pore emptying was due to evaporation (Kajama, 2015). Therefore, it can be concluded that N_2 adsorption/desorption on OPP and Mg-Fe LDH@OPP followed Type IV isotherm thus indicating

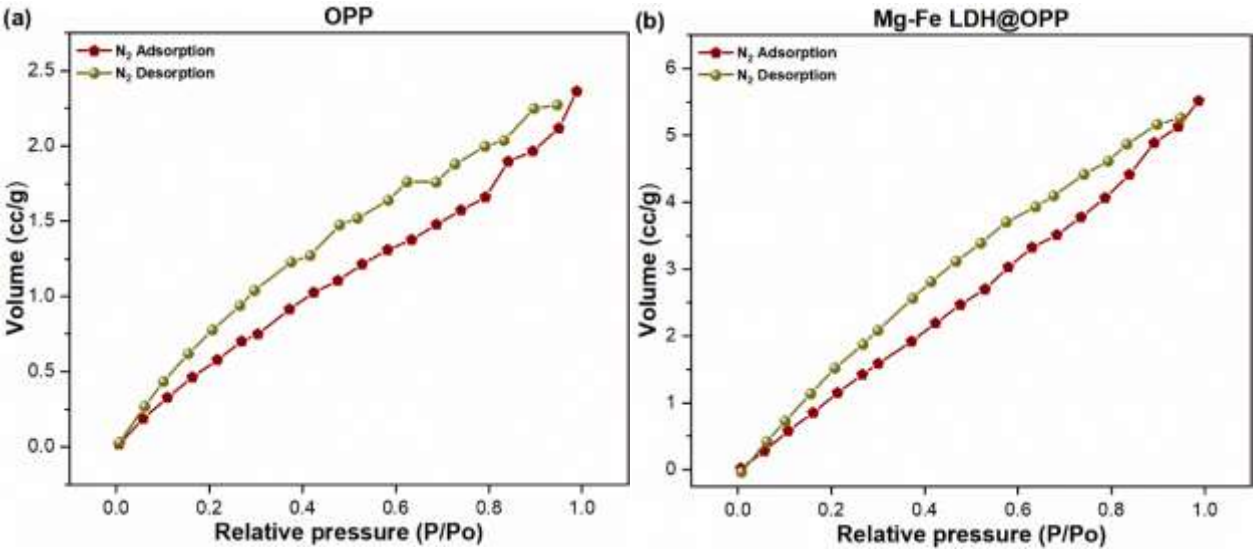

Figure 6: Nitrogen adsorption/desorptionisotherms of (a) OPP and (b) Mg-Fe LDH@OPP

mesoporous structural distribution.

4.1.5. XRD Analysis of OPP and Mg-Fe LDH@OPP

The XRD analysis of OPP and Mg-Fe LDH@OPP was conducted to obtain information regarding the structure, phase, crystal orientation and lattice parameters of the adsorbents. The results of the analysis are given in **Figure 7**. The XRD analysis of OPP showed diffraction peaks on 2θ at 19.38° and 29.75°, 24.20° and 37.71°, indicating crystalline structures of hexagonal carbon (C_{70}) and (C) at plane (110) and (452) with JPCD card no. 48-1449 and 50-0927, hexagonal fullerene (C_{60}) at plane (002) with JPCD card no. 47-0787 and orthorhombic oxygen (O_2) at plane (111) with JPCD card no. 38-0903, respectively. Given their significance in the biosorbent composition of OPP, cellulose and lignin are predicted to be potential chemical compounds aiding the elimination of Cr (VI) from polluted water (Dey et al., 2021). A significant level of crystallinity was shown by the diffractogram of Mg-Fe LDH@OPP. While mapping the diffraction peak on 2θ at 15.22°, crystalline structures of hexagonal carbon (C_{70}) at plane (002) with JPCD card no. 48-1449 were seen, suggesting that Mg-Fe LDH@OPP form a rhombohedral shape as it crystallizes (Elmoubarki et al., 2017). Other diffraction peaks on 2θ at 21.40° and 38.22° were detected, showing crystalline structures of orthorhombic iron oxide (Fe_2O_3) at plane (112) with JPCD card no. 21-0920 and cubic magnesium oxide (MgO) at plane (400) with JPCD card no. 30-0794, respectively. The XRD analysis exhibited that the modification of OPP with Mg-Fe LDH resulted in the formation of three-dimensional arrangements of Mg and Fe, thus improving the crystallinity of the adsorbent (Benselka-Hadj Abdelkader et al., 2011). This may influence the surface area and porosity of the material, as well as the type and strength of interactions between the adsorbate molecules and the biosorbent's surface. This may also improve the sorption affinity of Mg-Fe LDH@OPP towards Cr (VI) anions from aqueous

matrices.The degree of crystallinity (DOC%) and crystallite size of the composite was calculated using **Equ. (11)** and **Equ. (12)** given in **Section 3.13.**(Falyouna et al., 2022). The DOC% of Mg-

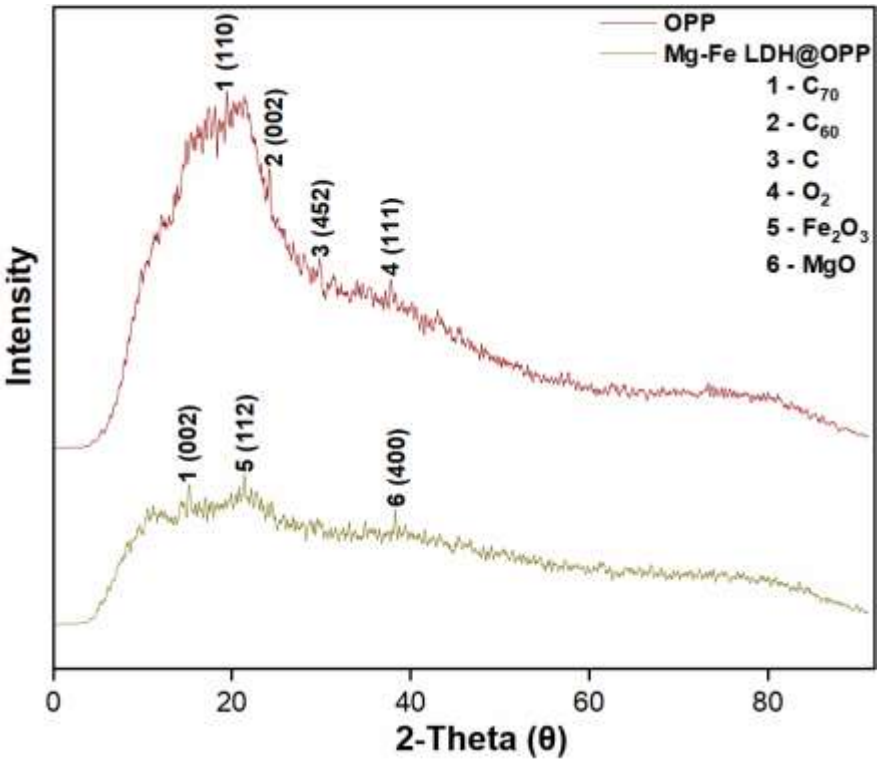

Figure 7: XRD analysis of OPP and Mg-Fe LDH@OPP

Fe LDH@OPP was calculated to be 2.32% while the crystallite size was 0.29 nm.

4.1.6. XRD Analysis of Mg-Fe LDH

Figure 8 presents the XRD analysis of Mg-Fe LDH. As presented in previous study(Nejati et al., 2014), the patterns fit well to layered double hydroxide with basal reflections of hkl planes (003), (006), (009), (110) and (113). The (003) reflection located on the 2θ of ~11.26° and 60° is typical of hydrotalcite-type materials, that indicates a basal spacing of ~0.78 nm, and is compatible with that in a nitrate containing LDH structure.

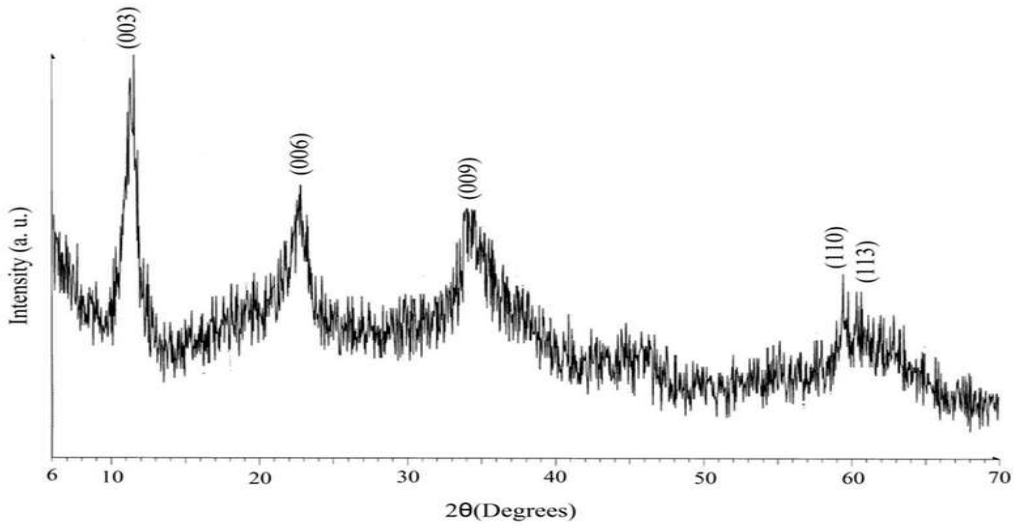

Figure 8: XRD analysis of Mg-Fe LDH

4.1.7. FT-IR Analysis

The results of FT-IR analysis of both adsorbents are presented in **Figure 9**. FT-IR spectrum of OPP revealed lignocellulosic characteristics of the material. The O-H and N-H groups' stretching found in carbohydrates, fatty acids and proteins are indicated in the wide band centered at 3422 cm^{-1}(Puccini et al., 2016). The COO^- groups of esters indicate the band at 1742 cm^{-1}(Puccini et al., 2016). Furthermore, C-O stretching is responsible for the bands at 1444 cm^{-1} and 1054 cm^{-1}(Puccini et al., 2016), which indicates typical bands of cellulose and hemicellulose from lignocellulosic materials. Similarly, in the case of Mg-Fe LDH@OPP, the bands observed at 3430 cm^{-1} and 1581 cm^{-1} are indicative of bending and stretching vibrations of OH groups (L. C. Santos et al., 2020). Similarly, M-O vibrations, where M is a stretching of either Mg or Fe, are connected to the band at 808 cm^{-1}(L. C. Santos et al., 2020). Furthermore, the band observed at 1358 cm^{-1} indicates the presence of CO_3^{2-} species on adsorbent surface, which may impair LDH's adsorption performance for contaminants in water (Meili et al., 2019). The FT-IR analysis showed that the COO^- and OH^- functional groups in both adsorbents may show dominant role in the contaminant removal process via complexation reactions.

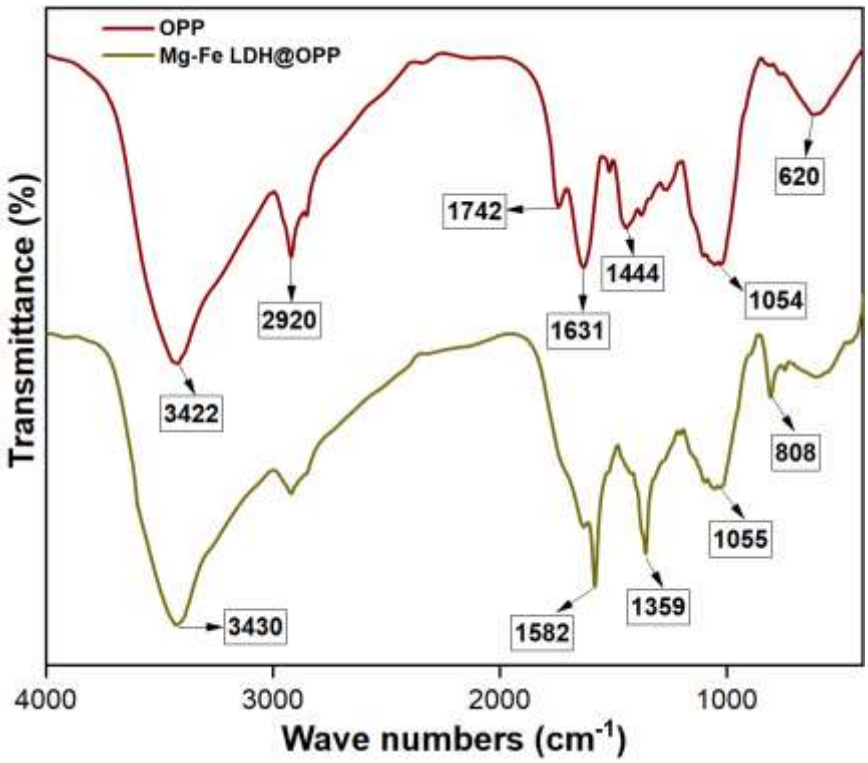

Figure 9: FT-IR analysis of OPP and Mg-Fe LDH@OPP

4.2. Batch Cr (VI) Sorption Studies

4.2.1. Influence of Dosages

Figure 10 depicts the performance of OPP and Mg-Fe LDH@OPP dosages in removing Cr (VI) from polluted water. It was found that the Cr (VI) sorption increases upon increasing dosages of both adsorbents. Upon increasing OPP and Mg-Fe LDH@OPP dosages from 0.1 g/L to 3 g/L, the Cr (VI) sorption varied from 31.72% to 85.93% and 36.53% to 94.27%, respectively. An inefficient Cr (VI) sorption performance at low adsorbent dosages may be ascribed to the large intraparticle distance between biosorbent and adsorbate, which resulted in relatively low diffusion of Cr (VI) ions onto the surfaces of OPP and Mg-Fe LDH@OPP (Padmavathy et al., 2016). At high dosages of both adsorbents, the intraparticle distance decreases, allowing for more efficient transfer of Cr (VI) ions towards the biosorbent surface and effectively sequestering Cr (VI) from aqueous media(Padmavathy et al., 2016). Moreover, better Cr (VI) sorption performance of Mg-Fe LDH@OPP was achieved, when compared with OPP. Such observation may be attributable to the availability of multiple activated groups on adsorbent surface induced by modification of OPP with bimetallic layered double hydroxide. Adding more, both adsorbents presented 100% Cr (VI) removal at 5 g/L dosage. Conversely, the adsorption capacity of OPP and Mg-Fe LDH@OPP for Cr (VI) showed significant decline from 63.45 mg/g to 5.72 mg/g and 73.07 mg/g to 6.28 mg/g, respectively upon increasing adsorbent dosages from 0.1 g/L to 3 g/L, as can be observed in **Figure 10**. The decrease in sorption capacity suggested that as adsorbent dosages increased, the residual Cr (VI) concentration

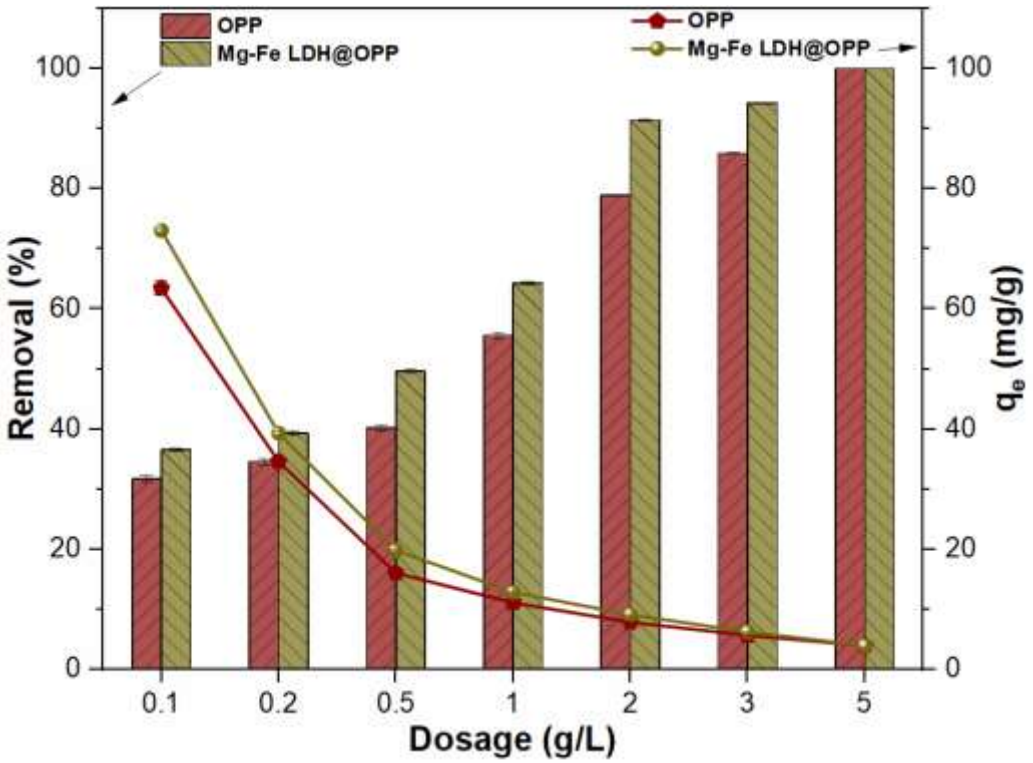

Figure 10: Influence of adsorbent dosage on the adsorption behavior of OPP and Mg-Fe LDH@OPP

sequestered per unit dosages of OPP and Mg-Fe LDH@OPP decreased, indicating more available surface sites for removing Cr (VI) under such water conditions (Inam et al., 2018). At 5 g/L dosages of both adsorbent, 4 mg/g adsorption capacity was observed. Considering removal efficiency 78.90% and 91.41% and adsorption capacity 7.89 mg/g and 9.14 mg/g, 2 g/L of OPP and Mg-Fe LDH@OPP dosages were used for subsequent experiments.

4.2.2. Influence of pH

pH is one of the most influential water chemistry factors that determine the sorption performance of a system. As shown in **Figure 11**, the removal performance of OPP and Mg-Fe LDH@OPP for Cr (VI) decreases from 78.90% to 32.98% and 91.41% to 41.51%, respectively upon increasing pH (2 to 9) of working solutions. Conversely, adsorption capacity also decreases for both adsorbents from 7.89 mg/g to 3.29 mg/g and 9.14 mg/g to 4.15 mg/g, respectively.

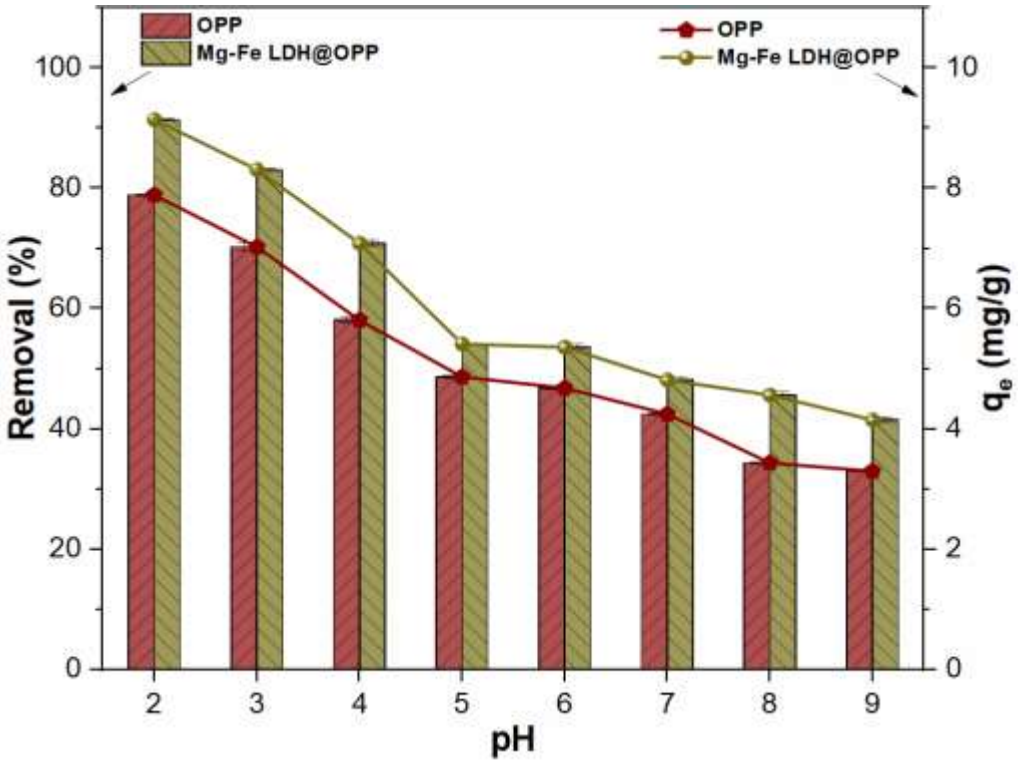

Figure 11: Influence of pH on the adsorption behavior of OPP and Mg-Fe LDH@OPP

4.2.2.1. Cr (VI) Speciation Diagram

As shown in **Figure 12**, at acidic pH conditions (< 6.3), Cr (VI) exists in two forms i.e., $HCrO_4^-$ and $Cr_2O_7^{2-}$ which may tend to get sorbed to positively charged OPP and Mg-Fe LDH@OPP surface because of charge neutralization (Shakya et al., 2019). The decreasing trend in adsorption capacity of both adsorbent for Cr (VI) at pH values < 6.3 may be ascribed to the fact that $HCrO_4^-$ has one anionic exchangeable site and $Cr_2O_7^{2-}$ has two anionic exchangeable sites, and that the fraction of later Cr (VI) specie increases with pH, thus posing significant impact on Cr (VI) removal process (Kane et al., 2016; Kuppusamy et al., 2016). However, the adsorption performance of both adsorbents for Cr (VI) continuously declined after pH 6 because at higher pH (> 6.3), Cr (VI) mainly exists as CrO_4^{2-}(Shakya et al., 2019). Upon increasing pH values to alkaline conditions, where pH > pH_{pzc} (OPP: 3.3; Mg-Fe LDH@OPP: 4.7), further decline in Cr (VI) sorption may be ascribed to the presence of higher quantity of negatively charged OH^- ions that compete with Cr (VI) for active sorption sites. Moreover, the dominant role of electrostatic repulsive forces may also affect the adsorption performance of both adsorbents at higher pH conditions. Therefore, subsequent experiments were conducted at acidic pH 2 to monitor sorption performance of OPP and Mg-Fe LDH@OPP in heterogeneous water matrices.

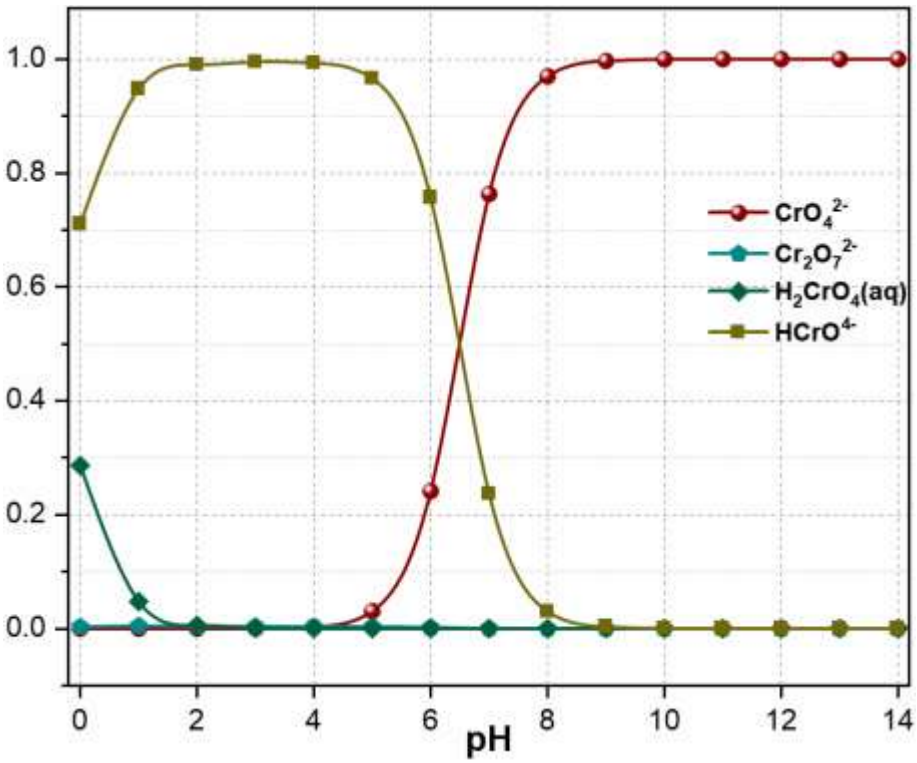

Figure 12: Cr (VI) speciation diagram

4.2.3. Influence of Contact Time

Figure 13 shows the removal efficiency and sorption capacity of OPP and Mg-Fe LDH@OPP at different time intervals. The results showed that Cr (VI) sorption efficiency increased for OPP from 72% to 78.9% and Mg-Fe LDH@OPP from 84.3% to 91.41% at time intervals of 30 min to 120 min. Upon further increasing contact time to 180 min, OPP and Mg-Fe LDH@OPP presented maximum removal as 81.84% and 100%, respectively. Such highly efficient Cr (VI) removal performance of Mg-Fe LDH@OPP may be related to its improved surface characteristics as compared to OPP as evidenced by BET analysis, shown in **Table 2**. The Cr (VI) sorption was not improved by extending contact time to 240 min for either absorbent. Conversely, a similar trend in sorption capacity of OPP (up to 8.18 mg/g) and Mg-Fe LDH@OPP (10 mg/g) for Cr (VI) was observed. These results may be ascribed to the fact that increasing contact time may increase Cr (VI) diffusive property towards sorbent surface, thus leading to effective Cr (VI) remediation performance from aqueous matrices (Al-Ghouti & Al-Absi, 2020).

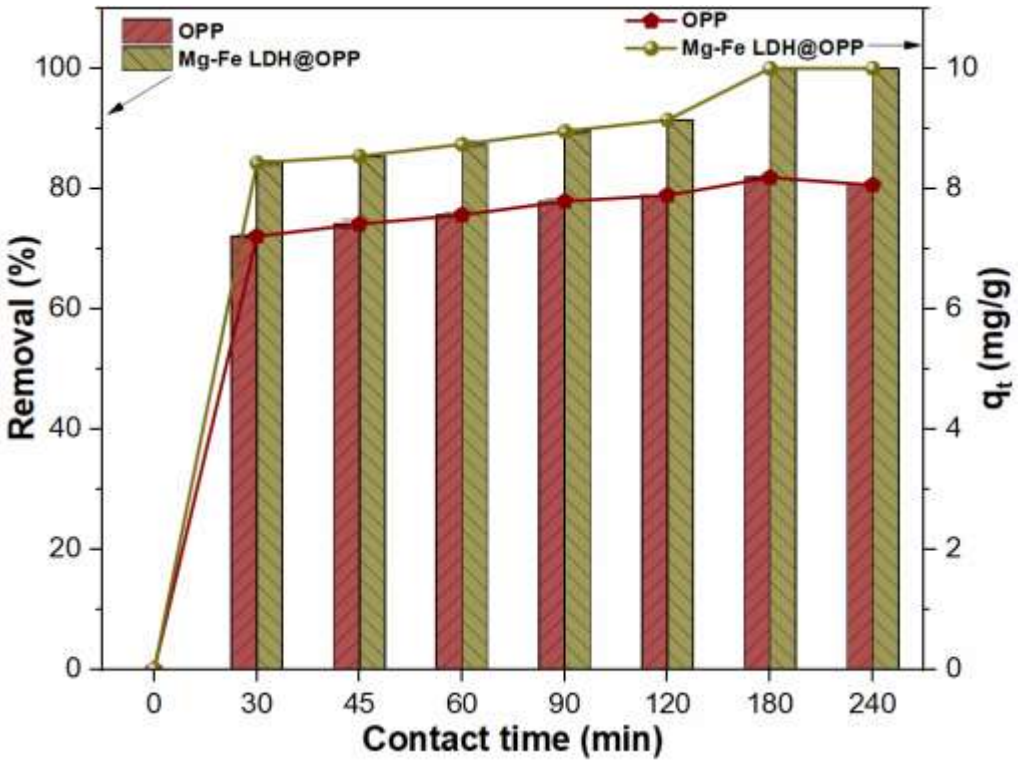

Figure 13: Influence of contact time on removal efficiency of OPP and Mg-Fe LDH@OPP

4.2.3.1. Adsorption Kinetics

Pseudo second order (PSO) and pseudo first order (PFO) are two generally used kinetic models that can predict the rate of adsorption (Revellame et al., 2020). These models allow for the recognition of rate expressions that correspond to potential reaction mechanisms (Elmoubarki et al., 2017). Therefore, kinetic study was conducted by fitting experimental sorption data using PFO and PSO models, as presented in **Figure 14.**

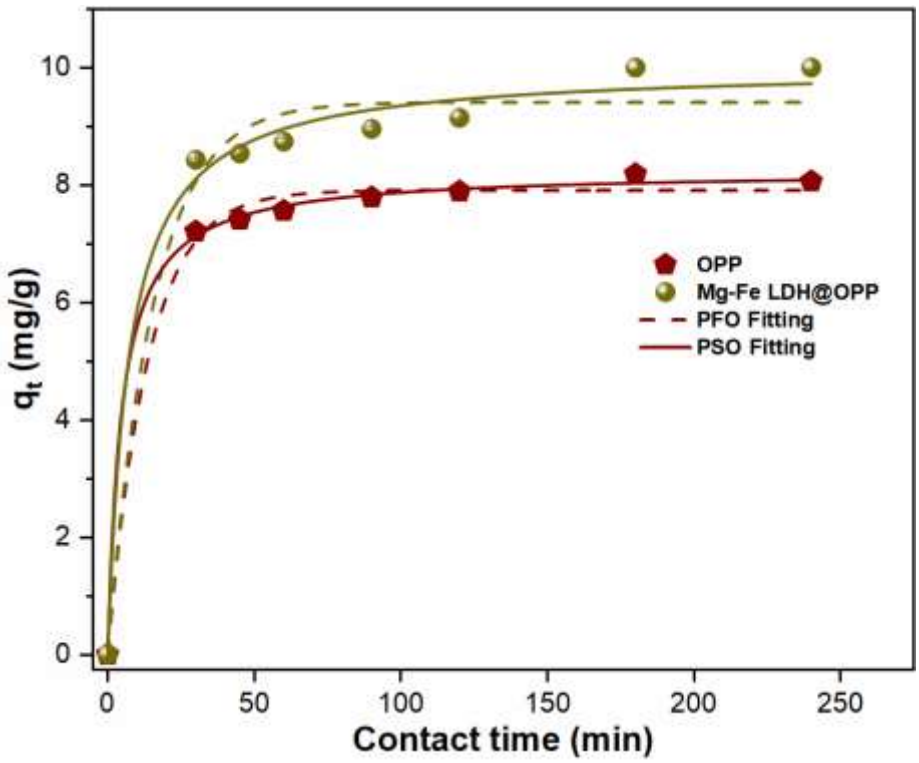

Figure 14: Kinetic studies of OPP and Mg-Fe LDH@OPP

The kinetic parameters' results are shown in **Table 3**. PSO model fitted better than PFO model, as regression coefficient R^2 values for OPP and Mg-Fe LDH@OPP were found greater i.e., 0.999 and 0.990 as compared to 0.994 and 0.977, respectively. Moreover, the experimental adsorption capacity at equilibrium time (180 min) was found closer to the modelled predicted value of PSO than PFO. Therefore, contact time (180 min) was selected for further batch-mode experiments. In addition, the results of kinetic model also suggested that sorption of Cr (VI) ions on both sorbents followed PSO model, thus indicating that chemisorption may play a dominant role as rate-limiting factor in Cr (VI) remediation from aqueous media (Elmoubarki et al., 2017).

Table 3: Parameters of adsorption kinetics of OPP and Mg-Fe LDH@OPP for Cr (VI) removal

Adsorbent	Pseudo-first order			Pseudo-second order		
	q_e (g/mol)	k_1 (1/min)	R^2	q_e (g/mol)	k_2 (mol/g.min)	R^2
OPP	7.907	0.073	0.994	8.242	0.025	0.999
Mg-Fe LDH@OPP	9.410	0.064	0.977	10.011	0.014	0.990

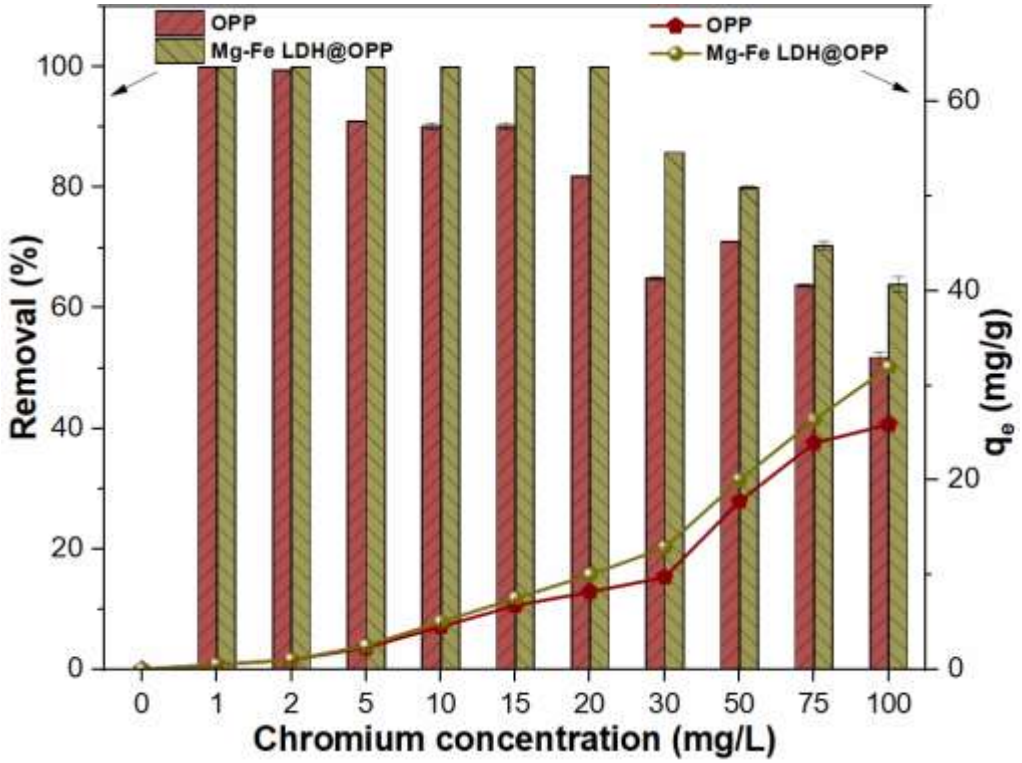

Figure 15: Influence of Cr (VI) concentration on removal efficiency of OPP and Mg-Fe LDH@OPP

4.2.4. Influence of Cr (VI) Concentration

Figure 15 demonstrates the sorption capacity and removal efficiency of OPP and Mg-Fe LDH@OPP at varying Cr (VI) concentrations in aqueous matrices. The results showed that Cr (VI) sorption efficiency decreased for OPP from 99.97% to 81.84% at varying Cr (VI) concentrations from 1 mg/L to 20 mg/L. In contrast, almost 100% Cr (VI) remediation was observed in the case of Mg-Fe LDH@OPP. Conversely, the sorption capacity of OPP and Mg-Fe LDH@OPP for Cr (VI) increased from 0.49 mg/g to 8.18 mg/g and 0.5 mg/g to 10 mg/g, respectively. The presence of bimetallic layered double hydroxides in Mg-Fe LDH@OPP as evidenced by SEM images may result in distinct Cr (VI) removal performance when compared with raw OPP, as shown in **Figure 2 and Figure 3**. The presence of higher Cr (VI) concentration (100 mg/L) in suspension caused a significant decrease in Cr (VI) removal performance (OPP: 51.76%; Mg-Fe LDH@OPP: 63.88%), as shown in **Figure 15**. This observation may be attributed to the presence of limited active sites, which may reduce the Cr (VI) transport affinity from suspension to sorbent surface (Al-Ghouti & Al-Absi, 2020). Contrary to this, adsorption capacity increases to 25.88 mg/g and 31.94 mg/g for OPP and Mg-Fe LDH@OPP, respectively.

4.2.4.1. Adsorption Isotherms

Figure 16 demonstrates the graphical illustration of the isotherm studies of OPP and Mg-Fe LDH@OPP.

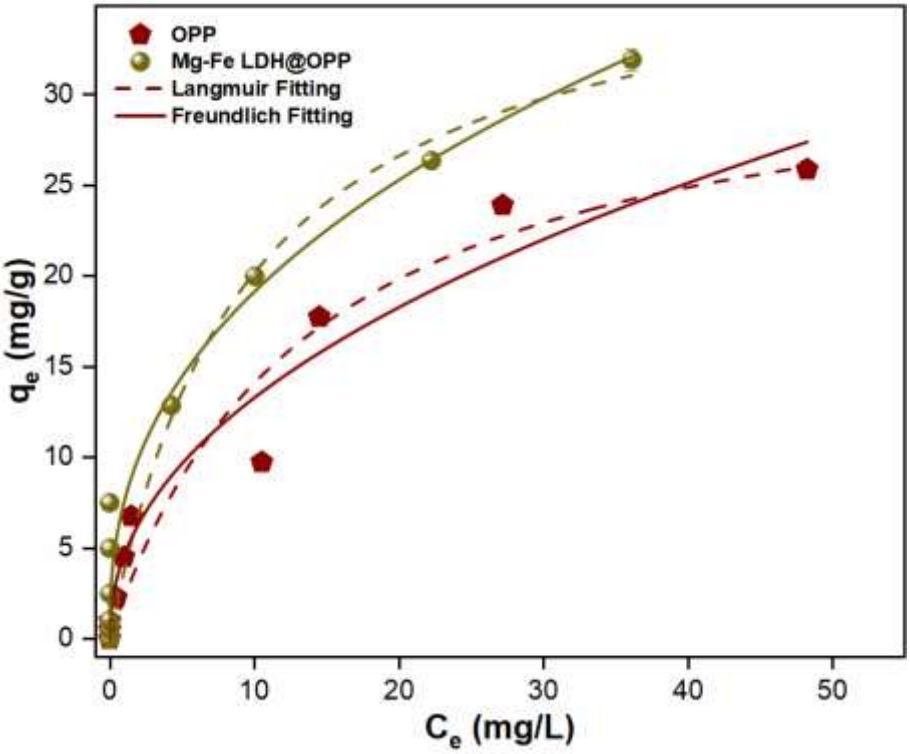

Figure 16: Isotherm studies of OPP and Mg-Fe LDH@OPP

The model parameters of isotherm studies are given in **Table 4**. Langmuir and Freundlich models were utilized to assess the sorption of Cr (VI) on the adsorbents' surface. The R^2 values of Freundlich model (OPP: 0.958; Mg-Fe LDH@OPP: 0.916) was observed to be slightly better than Langmuir model (OPP: 0.941; Mg-Fe LDH@OPP: 0.915). These results suggest the prominent role of multilayer Cr (VI) sorption onto heterogeneous sorption sites of both sorbents (Irem et al., 2017).

Table 4: Parameters of adsorption isotherms of OPP and Mg-Fe LDH@OPP for Cr (VI) removal

Isotherm models	Adsorbent	Parameters		R^2
Langmuir		q_m (g/mol)	K_L (L/mg)	
	OPP	34.981	0.063	0.941
	Mg-Fe LDH@OPP	39.146	0.106	0.915
Freundlich		N	K_F $[(g/mol)(L/mg)]^{1/n}$	
	OPP	2.185	4.648	0.958
	Mg-Fe LDH@OPP	2.481	7.567	0.916

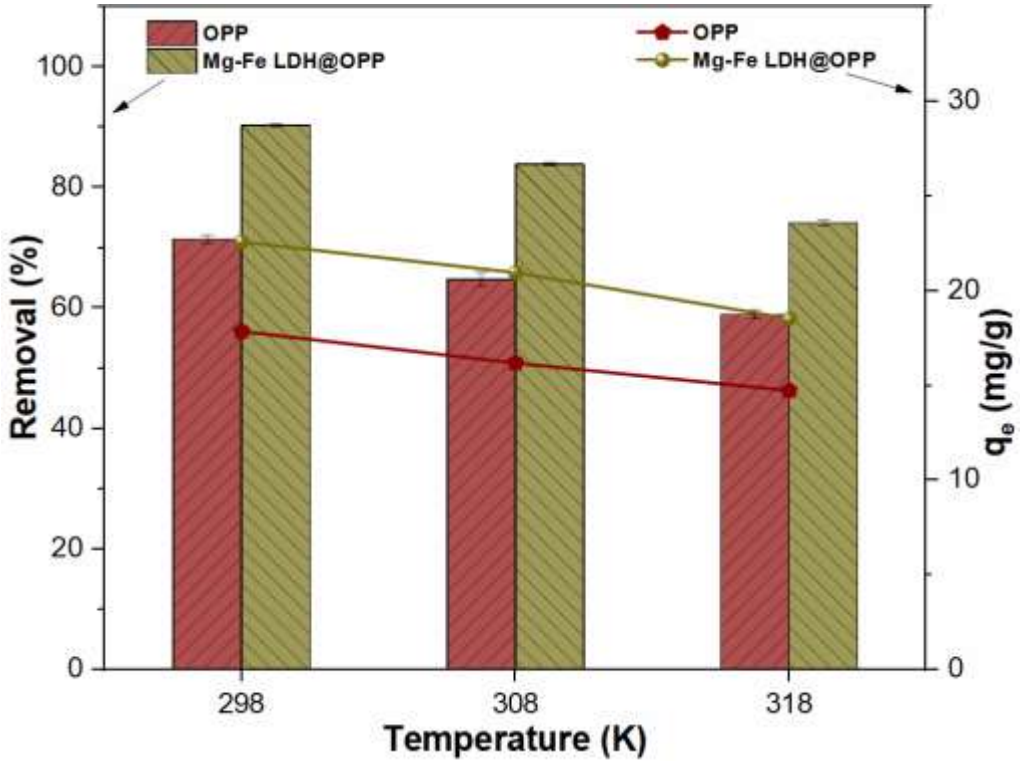

Figure 17: Influence of temperature on removal efficiency of OPP and Mg-Fe LDH@OPP

4.2.5. Influence of Temperature

Figure 17presents the sorption capacity and removal efficiency of OPP and Mg-Fe LDH@OPP at different suspension temperatures. The outcomes implied that Cr (VI) sorption efficiency decreased for OPP from 71.42% to 58.90% and Mg-Fe LDH@OPP from 90.33% to 74.16% at varying suspension temperatures from 298 K to 318 K. Conversely, a similar decreasing trend in adsorption capacity of OPP from 17.85 mg/g to 14.72 mg/g and Mg-Fe LDH@OPP from 22.58 mg/g to 18.54 mg/g for Cr (VI) with varying suspension temperatures was observed. Such observation may be related to the increase in thermal energy, which may disrupt the attractive forces between the biosorbents and Cr (VI) ions, making it easier for the ions to desorb from the surface of OPP and Mg-Fe LDH@OPP and return to the solution (Jnr & Spiff, 2005; Mustapha et al., 2019).

4.2.5.1. Adsorption Thermodynamics

To further investigate the adsorption characteristics, thermodynamic parameters were calculated by plotting the graph between ΔG and suspension temperatures, as shown in **Figure 18**.

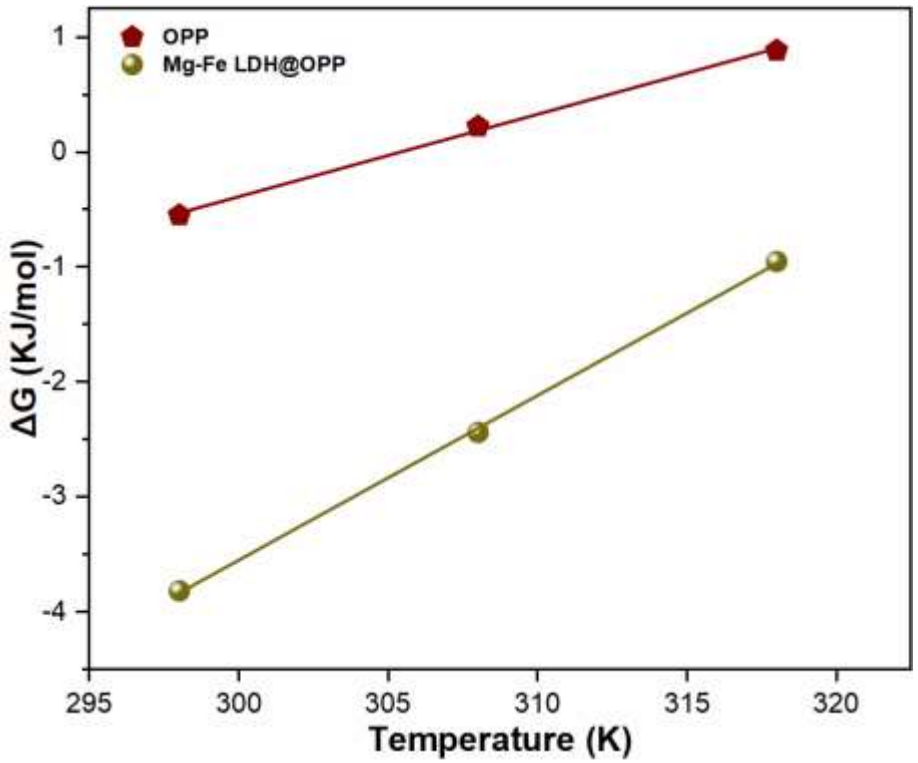

Figure 18: Thermodynamics studies of OPP and Mg-Fe LDH@OPP

The values of ΔS and ΔH were calculated using slope and intercept, as shown in **Table 5**. The negative values of ΔG at 298 K in case of OPP and at 298 K to 318 K in case of Mg-Fe LDH@OPP suggests that adsorption was spontaneous process. The progressive rise in ΔG value with temperature indicates that the increase in temperature has an adverse effect on the adsorption affinity of both adsorbents. The negative ΔH values also confirms that the elimination of Cr (VI) by both sorbents was exothermic process (Georgieva et al., 2020). Furthermore, the increasing randomness of the heterogeneous sites during the sorption phase may be indicated by the positive ΔS values (Inam et al., 2021). Furthermore, the absolute ΔH values (OPP: 21.88; Mg-Fe LDH@OPP: 46.50) suggested that both physical adsorption and complexation reaction might occur during Cr (VI) removal from water. This finding is consistent with previous research, which suggest that the absolute ΔH value if lies in the range of 0-8 KJ/mol represents physisorption, in the range of 8-60 KJ/mol represents physicochemical sorption and in the range of > 60 KJ/mol represents chemisorption phenomena (Chaudhry et al., 2017).

Table 5: Parameters of thermodynamic studies

Temperature (K)	ΔG (KJ/mol)	ΔH (KJ/mol)	ΔS (KJ/mol.K)	R^2
		OPP		
298	-0.55233	-21.88143	0.07164	0.99594
308	0.22003			
318	0.880408			
		Mg-Fe LDH@OPP		
298	-3.819004787	-46.50076	0.14317	0.99906
308	-2.441089856			
318	-0.955660094			

4.2.6. Influence of Interfering Ions

The presence of co-existing ions may influence the Cr (VI) removal potential, probably due to its competition for adsorption sites on the surface of OPP and Mg-Fe LDH@OPP. Therefore, Cr (VI) sorption potential was examined in the presence of PO_4^{3-}, NO_3^-, SO_4^{2-}, Cl^- and HCO_3^- at varying pH conditions of 2, 4 and 6 in aqueous medium, as shown in **Figure 19**. The results indicated that presence of interfering anions impart similar Cr (VI) removal trend as the absence of such species under varying pH conditions. Moreover, the Cr (VI) removal potential of both OPP and Mg-Fe LDH@OPP was insignificantly affected in the presence of NO_3^-, SO_4^{2-} and Cl^-, suggesting that these ions didn't interact strongly with Cr (VI) ions for adsorption sites (Akram et al., 2022). Similarly, slight influence of PO_4^{3-} anions on Cr (VI) sorption potential was perceived under the application of Mg-Fe LDH@OPP, which may be attributable to availability of sufficient adsorption sites (Akram et al., 2022). However, reduction in Cr (VI) sorption potential up to 13% was observed in the presence of PO_4^{3-} ions when using OPP as an adsorbent. Similarly, an inhibitory effect on Cr (VI) remediation was perceived in the presence of HCO_3^- species for suspensions treated with both OPP and Mg-Fe LDH@OPP. This behavior could be attributable to the fact that both species are anionic, which means they compete for the adsorbent's positively charged surface, lowering the likelihood of Cr (VI) remediation from water (Zhou et al., 2017).

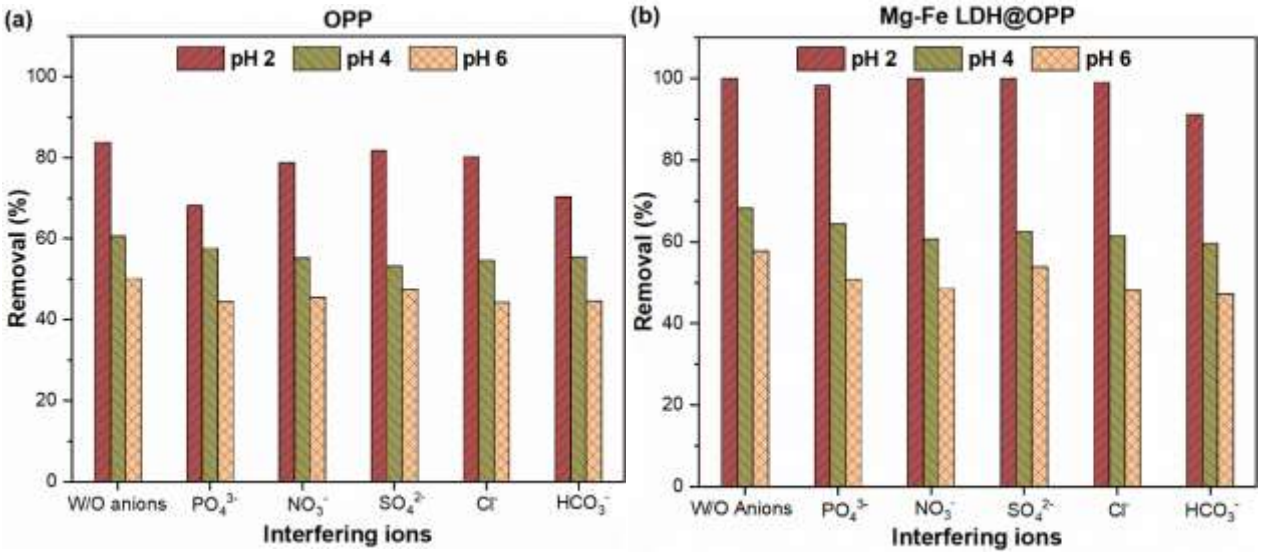

Figure 19: Cr (VI) removal potential using OPP and Mg-Fe LDH@OPP under the influence of interfering ions

4.2.7. Regeneration Cycle

Figure 20presents the regeneration performance of OPP and Mg-Fe LDH@OPP over five adsorption/desorption cycles. A substantial decline in the Cr (VI) sorption up to 7.01% and 23.26% was observed for OPP and Mg-Fe LDH@OPP, respectively, at the fifth cycle. Similarly, the sorption capacity also decreased to 0.7 mg/g and 2.32 mg/g for both adsorbents. This decline might be tied to the fact that the sorption capacity of the adsorbents is not infinite, and with each cycle, the adsorbents become saturated with Cr (VI) ions, reducing the surface area available for additional adsorption in subsequent cycles, thus leading to a decrease in the sorption affinity(El-Bendary et al., 2022). Furthermore, as the Cr (VI) ions accumulate on the surface of OPP and Mg-Fe LDH@OPP, they may alter the adsorbents' surface properties, thus leading to decrease in adsorption potential after each cycle. Also, with repeated use, the adsorbent surface may undergo degradation, which may reduce its surface area and affect its adsorption ability, leading to a reduction of adsorption performance in subsequent cycles (Gkika et al., 2022).

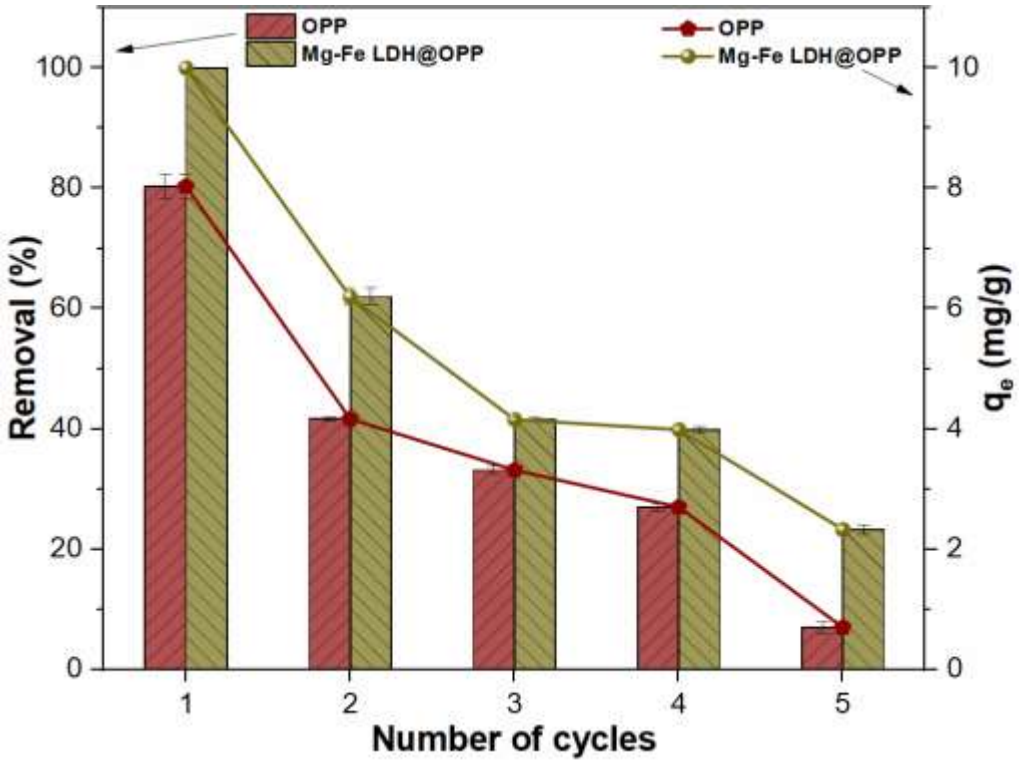

Figure 20: Regeneration cycles of OPP and Mg-Fe LDH@OPP for Cr (VI) removal

4.3. Fixed Bed Column Studies

Figure 21(a, b) displays the breakthrough curves at bed depths of 0.5 cm and 1.0 cm, respectively. It was perceived that increase in bed depth enhances Cr (VI) removal efficiency with significantly better performance in case of Mg-Fe LDH@OPP than OPP. In addition, the column exhaustion time was also found to be greater for Mg-Fe LDH@OPP (600-800 min) than OPP (100-350 min), thus indicating its applicability for long term operation. Such performance may be supported by the results of BET, morphological and elemental composition analysis, which showed large surface area, uneven particle distribution and greater particle size in Mg-Fe LDH@OPP composite, as discussed in **Section 4.1.1**.

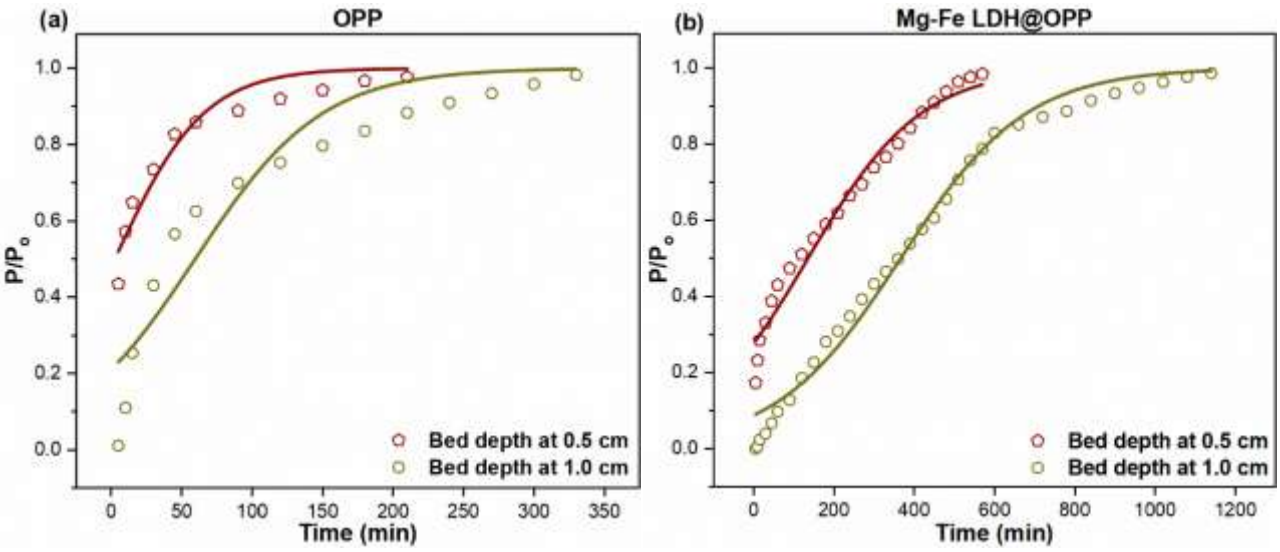

Figure 21: Cr (VI) breakthrough curve of (a) OPP and (b) Mg-Fe LDH@OPP

The experimental data was fitted with the Yoon-Nelson model to examine the breakthrough time of column. The slope and intercept of Yoon-Nelson plot was used to estimate the values T (time required for 50% Cr (VI) breakthrough) and of K_{YN} (rate constant), as presented in **Table 6** in the supplementary section. It was observed that with the increase in bed depth, values of K_{YN} decreases while the value of T increases. Moreover, the breakthrough times were observed to be 3 and 60 min for OPP, and 135 and 366 min for Mg-Fe LDH@OPP, respectively with the bed depth of 0.5 cm and 1.0 cm. Such observation might be related to the fact that as bed depth increases, the rate at which the adsorbent bed is exhausted decreases. Similarly, previous studies(Mekonnen et al., 2021; Omitola et al., 2022) also presented better adsorption performance of contaminants at higher bed depths of adsorbents within the column. The experimental data was likewise shown to be well fitted by the Yoon-Nelson model, with correlation coefficients (R^2) in the ranges of 0.8849-0.9250 for OPP and 0.9753-0.9867 for Mg-Fe LDH@OPP, respectively, as shown in **Table 6** in the supplementary section.

Table 6: Parameters of fixed bed column studies

Bed Depth (cm)	K_{YN} (min^{-1})	T (min)	R^2
OPP			
0.5	0.03186	2.54492	0.92503
1.0	0.02221	59.50934	0.88494
Mg-Fe LDH@OPP			
0.5	0.00711	135.45931	0.97533
1.0	0.0064	366.37962	0.98671

4.4. Adsorption Mechanism

The sorption mechanism of Cr (VI) ions onto OPP and Mg-Fe LDH@OPP was identified based on experimental results, mathematical models, and spectroscopic techniques. For instance, at acidic pH conditions, both adsorbents presented excellent Cr (VI) removal potential owing to strong electrostatic attraction between negatively charged Cr (VI) ions and positively charged biosorbent surface(Shakya et al., 2019). However, decreasing trend in Cr (VI) removal potential with pH may be linked with the pH_{pzc} values (OPP: 3.3 and Mg-Fe LDH@OPP: 4.7). Therefore, a significant decline in Cr (VI) remediation performance was noted at alkaline pH conditions, as shown in **Figure 11**. Moreover, studies on sorption kinetics, isotherms, and thermodynamics were conducted to better predict the Cr (VI) remediation process using OPP and Mg-Fe LDH@OPP. It was observed that multilayered chemisorption processes, along with physisorption and complexation reactions resulted in enhanced Cr (VI) remediation from aqueous media(Chaudhry et al., 2017; Elmoubarki et al., 2017; Georgieva et al., 2020; Inam et al., 2021; Irem et al., 2017).To get further mechanistic insight into the Cr (VI) sorption, XRD and FT-IR analysis were carried out after interaction of Cr (VI) ions with OPP and Mg-Fe LDH@OPP.

4.4.1. XRD of Spent Adsorbent

The XRD analysis of spent OPP and Mg-Fe LDH@OPP presented the appearance of new diffraction peaks and disappearance of some old diffraction peaks, as shown in **Figure 22**. For instance, in the case of spent OPP, new diffraction peaks were observed on 2θ at 14.83° indicating crystalline structure of orthorhombic chromium carbonyl ($Cr(CO)_6$) at plane (231) with JPCD card no. 40-0751, while two new peaks of hexagonal chromium carbide (Cr_7C_3) at plane (421) with JPCD card no. 11-0550, were observed on 2θ at 63.94° and 81.17°.As presented in previous study(Zhang et al., 2017), Cr_7C_3 is complex compound containing Cr and Cr_2O_3 which indicates presence of reduced Cr(III) species on spent OPP. For spent Mg-Fe LDH@OPP, new peaks were observed on 2θ at 21°, 30°, 35.8° and 43.55°, indicating crystalline structures of orthorhombic chromium oxalate (CrC_2O_4) at plane (011) with JPCD card no. 45-0896, tetragonal iron chromite ($FeCr_2O_4$) at plane (311) with JPCD card no. 4-0511, cubic iron oxalate (FeC_2O_4) at plane (311) with JPCD card no. 14-0807 and tetragonal chromium magnesium oxide (Cr_2MgO_4) at plane (311) with JPCD card no. 20-0673, respectively. These results suggest the involvement of reduction of Cr (VI) to Cr (III) followed by adsorption onto OPP and Mg-Fe LDH@OPP surface. Similarly, previous study (Z. Li et al., 2023) also indicated that variation in electronic binding energies of iron and oxygen atoms as well as -OH functional groups on adsorbent surface were mainly responsible for reduction of Cr (VI) to Cr (III) during sorption process.

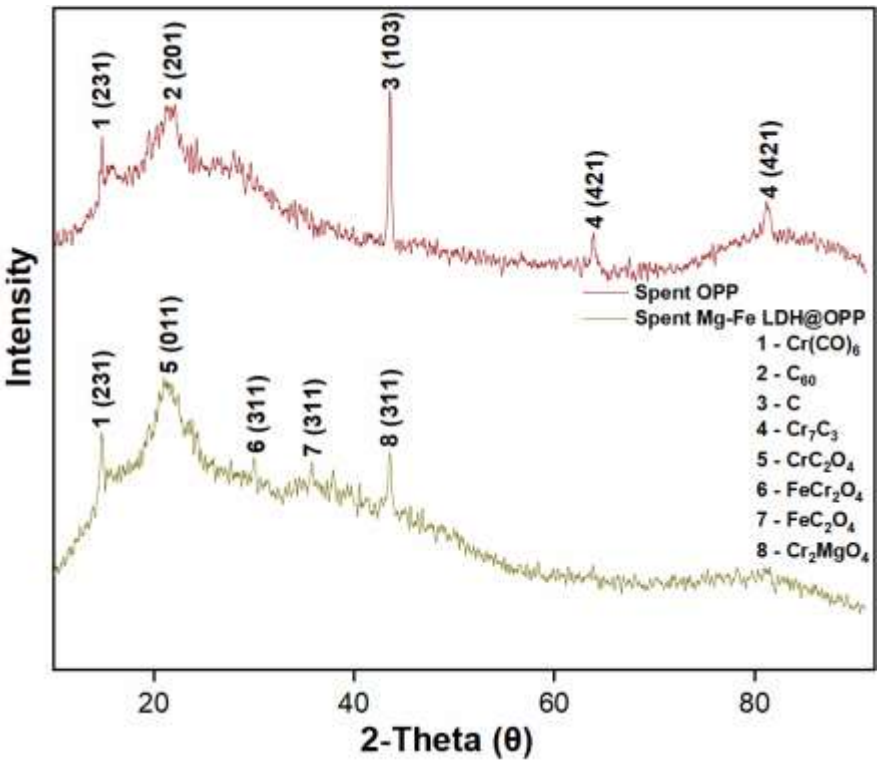

Figure 22: XRD of spent OPP and Mg-Fe LDH@OPP

4.4.2. FT-IR of Spent Adsorbent

The results of the FT-IR study showed that distinct complexation processes between Cr (VI) and adsorbents had a role in the disappearance, appearance and shifting of different peaks, as shown in **Figure 23**. For instance, in the case of spent OPP, the disappearance of COO^- groups of esters at 1742 cm^{-1} may be attributable to the bond formation between COO^- and Cr (VI) ions via ligand exchange (Inam et al., 2019). Similarly, the disappearing of C-O stretching vibration peaks at 1444 cm^{-1} and 1053 cm^{-1} was also observed, indicating the possibility of physical adsorption (Inam et al., 2019). However, in the case of spent Mg-Fe LDH@OPP, disappearance of peak at 808 cm^{-1} and appearance of new peak at 541 cm^{-1} was observed, thus indicating involvement of C-H bending vibrations in Cr (VI) removal process. In contrast, the change in intensity of other peaks were observed thus highlighting the involvement of complexation processes.

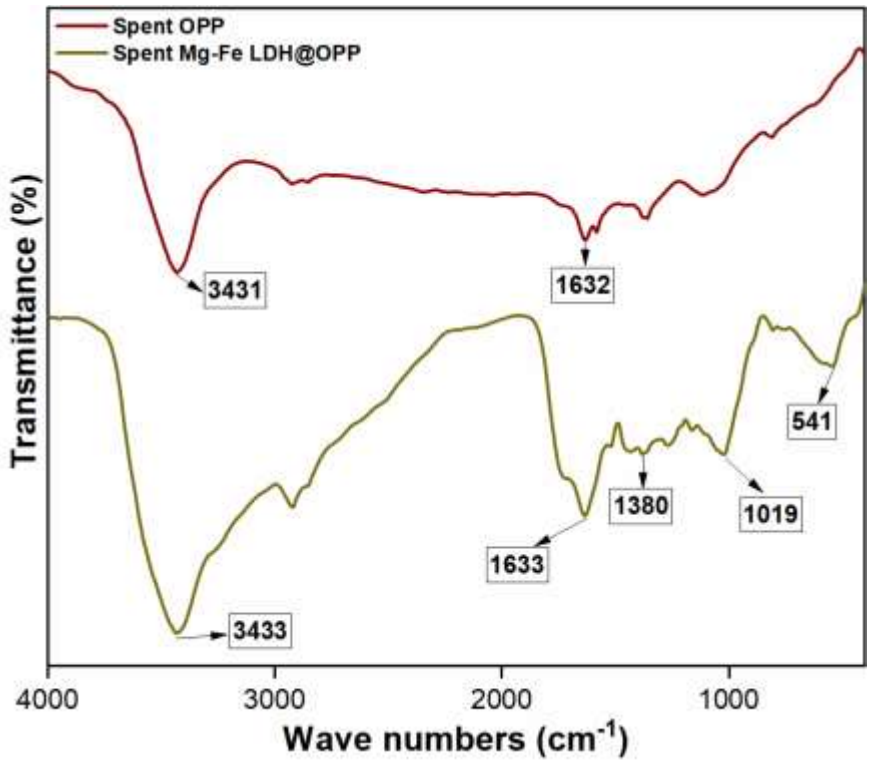

Figure 23: FT-IR of spent OPP and Mg-Fe LDH@OPP

These results suggested that governing removal process involved in Cr (VI) removal using Mg-Fe LDH@OPP was identified as physical adsorption, chemisorption, reduction, and complexation reactions. However, in addition to these mechanisms, the involvement of ligand exchange resulted in Cr (VI) removal using OPP. The pictorial illustration of proposed Cr (VI) removal mechanism using both adsorbents is also presented in **Figure 24**.

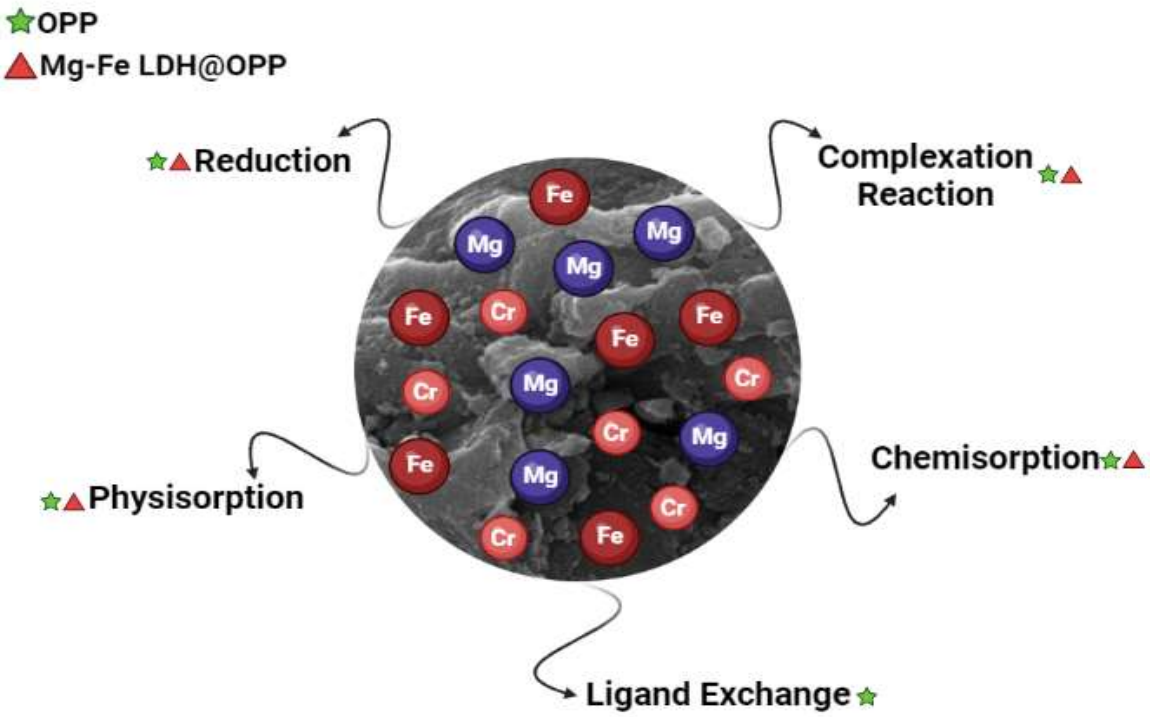

Figure 24: Pictorial illustration of Cr (VI) removal mechanism

4.5. Comparison of Contaminant with Literature Studies

Table 7indicates a comparison of Cr (VI) sorption capacity using different sorbents presented in previous research. The type of adsorbent and water chemistry parameters were closely related to adsorption capacity of Cr (VI) from various aqueous matrices. It can also be observed that relatively greater sorption capacities were observed for OPP (25.88 mg/g) and Mg-Fe LDH@OPP (31.94 mg/g) than other adsorbents studied in literature. Thus, it can be deduced that Mg-Fe LDH@OPP showed strong potential towards remediation of Cr (VI) species matrices with the possibility to be applied for pilot scale operation in water treatment.

Table 7: Comparison of contaminant with literature studies

Adsorbent	Dosage	Initial Cr (VI) Conc.	pH	Contact Time	Adsorption Capacity	Reference
	(g/L)	(mg/L)		(min)	(mg/g)	
Magnetite nanoparticles	6	60	3	120	7.2	(Padmavathy et al., 2016)
Magnetite graphene oxide nanocomposite	10	40	4	120	3.84	(Moges et al., 2022)
Potato peeling	4	40	2.5	48	10	(Mutongo et al., 2014)
Fox nutshell	0.5	10	2	180	19.8	(Kumar & Jena, 2017)
Moringa leaves	2.5	20	4.8	80	7.2	(Madhuranthakam et al., 2021)
Aloe vera leaves	2	50	1.23	150	24.66	(Prajapati et al., 2020)
Orange peel	1	10	2	150	8.9	(JishaTJ et al., 2017)
Orange peel powder	2	100	2	180	25.88	This study*
Mg-Fe LDH@OPP	2	100	2	180	31.94	This study*

CHAPTER 5

CONCLUSION AND RECOMMENDATIONS

5.1. Conclusion

The viability of Mg-Fe LDH@OPP was thoroughly explored as a novel biosorbent capable of removing Cr (VI) ions from water. The major findings drawn from the current research are as follows:

- Mg-Fe LDH@OPP presented superior Cr (VI) removal performance (100%) compared to raw OPP (81.84%) due to its increased particle size, uneven particle distribution, effective surface area and higher point of zero charge (pH_{pzc}).
- The kinetic models PFO and PSO satisfactorily explained the sorption of Cr (VI) ions onto OPP and Mg-Fe LDH@OPP, but the PSO model was better fitted with sorption data, as R^2 values of PSO model (OPP: 0.999; Mg-Fe LDH@OPP: 0.990) were found to be relatively greater than those for the PFO kinetic model (OPP: 0.994; Mg-Fe LDH@OPP: 0.977).
- The Freundlich isotherm primarily controlled Cr (VI) sorption onto OPP and Mg-Fe LDH@OPP, as indicated by its relatively greater R^2 values (OPP: 0.958; Mg-Fe LDH@OPP: 0.916) than Langmuir isotherm (OPP: 0.941; Mg-Fe LDH@OPP: 0.915).
- The thermodynamic characteristics showed that the physical adsorption and complexation reaction of Cr (VI) ions onto the surface of OPP and Mg-Fe LDH@OPP played significant roles in the removal process.
- The comparative better Cr (VI) removal performance of Mg-Fe LDH@OPP was also observed for up to five regeneration cycles and under the influence of interfering species in heterogeneous aqueous environment.
- Continuous mode column studies also indicated applicability of Mg-Fe LDH@OPP than raw OPP. The experimental data was also satisfactorily fitted with Yoon-Nelson model with R^2 values in the ranges of 0.8849-0.9250 for OPP and 0.9753-0.9867 for Mg-Fe LDH@OPP, respectively with bed depth of 0.5 cm and 1.0 cm, respectively.
- The main sorption mechanism involved in the removal of Cr (VI) by Mg-Fe LDH@OPP was determined to be physio-chemisorption, reduction, and complexation reactions. However, in addition to these mechanisms, the involvement of ligand exchange was also observed when remediating Cr (VI) species by OPP from aqueous solutions.

5.2. Recommendations

This study recommends that:

- The removal potential of other contaminants and heavy metals should be investigated using Mg-Fe LDH@OPP.
- The potential of other kinds of fruit and vegetable waste should be investigated to produce sustainable adsorbents.
- Real tannery wastewater should be used to investigate the removal efficiency of Mg-Fe LDH@OPP.

REFERENCES

Acar, F. N., & Malkoc, E. (2004). The removal of chromium(VI) from aqueous solutions by Fagus orientalis L. *Bioresource Technology*, *94*(1), 13–15. https://doi.org/10.1016/j.biortech.2003.10.032

AHMAD, S. W., ZAFAR, M. S., AHMAD, S., ZIA-UL-HAQ, M., ASHRAF, M., RABBANI, J., & ULLAH, S. (2020). Removal of chromium(VI) from wastewater through ion exchange. Kinetic and scale up studies. *Environment Protection Engineering*, *45*(1). https://doi.org/10.37190/epe190102

Akinhanmi, T. F., Ofudje, E. A., Adeogun, A. I., Aina, P., & Joseph, I. M. (2020). Orange peel as low-cost adsorbent in the elimination of Cd(II) ion: kinetics, isotherm, thermodynamic and optimization evaluations. *Bioresources and Bioprocessing*, *7*(1). https://doi.org/10.1186/s40643-020-00320-y

Akram, M., Gao, B., Pan, J., Khan, R., Inam, M. A., Xu, X., Guo, K., & Yue, Q. (2022). Enhanced removal of phosphate using pomegranate peel-modified nickel-lanthanum hydroxide. *Science of the Total Environment*, *809*. https://doi.org/10.1016/j.scitotenv.2021.151181

Al-Ghouti, M. A., & Al-Absi, R. S. (2020). Mechanistic understanding of the adsorption and thermodynamic aspects of cationic methylene blue dye onto cellulosic olive stones biomass from wastewater. *Scientific Reports*, *10*(1). https://doi.org/10.1038/s41598-020-72996-3

Amuda, O. S., Amoo, I. A., & Ajayi, O. O. (2006). *Coagulation/flocculation Process In The Removal Of Trace Metals Present In Industrialwastewater Geochemical Characterization of Soil in the Bitumen Environment of Ondo State, Southwestern Nigeria View project TWAS CSIR View project*. https://www.researchgate.net/publication/284509397

Ayele, A., & Godeto, Y. G. (2021). Bioremediation of Chromium by Microorganisms and Its Mechanisms Related to Functional Groups. In *Journal of Chemistry* (Vol. 2021). Hindawi Limited. https://doi.org/10.1155/2021/7694157

Barnhart, J. (1997). Occurrences, Uses, and Properties of Chromium. In *REGULATORY TOXICOLOGY AND PHARMACOLOGY* (Vol. 26).

Barrera-Díaz, C. E., Lugo-Lugo, V., & Bilyeu, B. (2012). A review of chemical, electrochemical and biological methods for aqueous Cr(VI) reduction. In *Journal of Hazardous Materials* (Vols. 223–224, pp. 1–12). https://doi.org/10.1016/j.jhazmat.2012.04.054

Basavaraju, P., & Ramakrishnaiah, C. R. (2012). *Hexavalent chromium removal from industrial waste water by chemical precipitation method HEXAVALENT CHROMIUM REMOVAL FROM INDUSTRIAL WATSEWATER BY CHEMICAL PRECIPITATION METHOD*. www.ijera.com

Benselka-Hadj Abdelkader, N., Bentouami, A., Derriche, Z., Bettahar, N., & de Ménorval, L. C. (2011). Synthesis and characterization of Mg-Fe layer double hydroxides and its application on adsorption of Orange G from aqueous solution. *Chemical Engineering Journal*, *169*(1–3), 231–238. https://doi.org/10.1016/j.cej.2011.03.019

Bianchi, V., Celotti, L., Lanfranchi, G., Majone, F., Marin, G., Montaldi, A., Sponza, G., Tamino, G., Venier, P., Zantedeschi, A., & Levis, A. G. (1983). Genetic effects of chromium compounds. In *Mutation Research* (Vol. 117).

Bishnoi, N. R., Bajaj, M., Sharma, N., & Gupta, A. (2004). Adsorption of Cr(VI) on activated rice husk carbon and activated alumina. *Bioresource Technology*, *91*(3), 305–307. https://doi.org/10.1016/S0960-8524(03)00204-9

Bregnbak, D., Johansen, J. D., Jellesen, M. S., Zachariae, C., Menné, T., & Thyssen, J. P. (2015). Chromium allergy and dermatitis: Prevalence and main findings. In *Contact Dermatitis* (Vol. 73, Issue 5, pp. 261–280). https://doi.org/10.1111/cod.12436

Carneiro, M. A., Pintor, A. M. A., Boaventura, R. A. R., & Botelho, C. M. S. (2022). Efficient removal of arsenic from aqueous solution by continuous adsorption onto iron-coated cork granulates. *Journal of Hazardous Materials*, *432*. https://doi.org/10.1016/j.jhazmat.2022.128657

Chandio, T. A., Khan, M. N., Muhammad, M. T., Yalcinkaya, O., Turan, E., & Kayis, A. F. (2021). *Health risk assessment of chromium contamination in the nearby population of mining plants, situated at Balochistan, Pakistan*. https://doi.org/10.1007/s11356-020-11649-4/Published

Chandravanshi, B. S., & Leta, S. (2017). *Chemical precipitation method for chromium removal and its recovery from tannery wastewater in Ethiopia Municipal wastewater treatment View project Levels of selected metals in the leaves of Ruta chalepensis L. (Rue) collected from four different areas of Ethiopia View project*. https://www.researchgate.net/publication/316601925

Chaudhry, S. A., Zaidi, Z., & Siddiqui, S. I. (2017). Isotherm, kinetic and thermodynamics of arsenic adsorption onto Iron-Zirconium Binary Oxide-Coated Sand (IZBOCS): Modelling and process optimization. *Journal of Molecular Liquids*, *229*, 230–240. https://doi.org/10.1016/j.molliq.2016.12.048

Çimen, A. (2015). Removal of chromium from wastewater by reverse osmosis. *Russian Journal of Physical Chemistry A*, *89*(7), 1238–1243. https://doi.org/10.1134/S0036024415070055

Danilov, F. I., Protsenko, V. S., Butyrina, T. E., Vasil'eva, E. A., & Baskevich, A. S. (2006). Electroplating of chromium coatings from Cr(III)-based electrolytes containing water soluble polymer. *Protection of Metals*, *42*(6), 560–569. https://doi.org/10.1134/S0033173206060075

Dev, S., Khamkhash, A., Ghosh, T., & Aggarwal, S. (2020). Adsorptive Removal of Se(IV) by Citrus Peels: Effect of Adsorbent Entrapment in Calcium Alginate Beads. *ACS Omega*, *5*(28), 17215–17222. https://doi.org/10.1021/acsomega.0c01347

Dey, S., Basha, S. R., Babu, G. V., & Nagendra, T. (2021). Characteristic and biosorption capacities of orange peels biosorbents for removal of ammonia and nitrate from contaminated water. *Cleaner Materials*, *1*. https://doi.org/10.1016/j.clema.2021.100001

Dos Santos, C. S. L., Miranda Reis, M. H., Cardoso, V. L., & De Resende, M. M. (2019). Electrodialysis for removal of chromium (VI) from effluent: Analysis of concentrated solution saturation. *Journal of Environmental Chemical Engineering*, *7*(5). https://doi.org/10.1016/j.jece.2019.103380

El-Bendary, N., El-Etriby, H. K., & Mahanna, H. (2022). Reuse of adsorption residuals for enhancing removal of ciprofloxacin from wastewater. *Environmental Technology (United Kingdom)*, *43*(28), 4438–4454. https://doi.org/10.1080/09593330.2021.1952310

Eljamal, O., Maamoun, I., Alkhudhayri, S., Eljamal, R., Falyouna, O., Tanaka, K., Kozai, N., & Sugihara, Y. (2022). Insights into boron removal from water using Mg-Al-LDH: Reaction parameters optimization & 3D-RSM modeling. *Journal of Water Process Engineering*, *46*. https://doi.org/10.1016/j.jwpe.2022.102608

Elmoubarki, R., Mahjoubi, F. Z., Elhalil, A., Tounsadi, H., Abdennouri, M., Sadiq, M., Qourzal, S., Zouhri, A., & Barka, N. (2017). Ni/Fe and Mg/Fe layered double hydroxides and their calcined derivatives: Preparation, characterization and application on textile dyes removal. *Journal of Materials Research and Technology*, *6*(3), 271–283. https://doi.org/10.1016/j.jmrt.2016.09.007

Enniya, I., Rghioui, L., & Jourani, A. (2018). Adsorption of hexavalent chromium in aqueous solution on activated carbon prepared from apple peels. *Sustainable Chemistry and Pharmacy*, *7*, 9–16. https://doi.org/10.1016/j.scp.2017.11.003

Falyouna, O., Bensaida, K., Maamoun, I., Ashik, U. P. M., Tahara, A., Tanaka, K., Aoyagi, N., Sugihara, Y., & Eljamal, O. (2022). Synthesis of hybrid magnesium hydroxide/magnesium oxide nanorods [Mg(OH)2/MgO] for prompt and efficient adsorption of ciprofloxacin from aqueous solutions. *Journal of Cleaner Production*, *342*. https://doi.org/10.1016/j.jclepro.2022.130949

Feng, N. C., Guo, X. Y., & Liang, S. (2010). Enhanced Cu(II) adsorption by orange peel modified with sodium hydroxide. *Transactions of Nonferrous Metals Society of China (English Edition)*, *20*(SUPPL.1). https://doi.org/10.1016/S1003-6326(10)60030-1

Forano, C., Costantino, U., Prévot, V., & Gueho, C. T. (2013). Layered double hydroxides (LDH). In *Developments in Clay Science* (Vol. 5, pp. 745–782). Elsevier B.V. https://doi.org/10.1016/B978-0-08-098258-8.00025-0

Gardea-Torresdey, J. L., Tiemann, K. J., Armendariz, V., Bess-Oberto, L., Chianelli, R. R., Rios, J., Parsons, J. G., & Gamez, G. (2000). Characterization of Cr(VI) binding and reduction to

Cr(III) by the agricultural byproducts of Avena monida (Oat) biomass. In *Journal of Hazardous Materials* (Vol. 80).

Genawi, N. M., Ibrahim, M. H., El-Naas, M. H., & Alshaik, A. E. (2020). Chromium removal from tannery wastewater by electrocoagulation: Optimization and sludge characterization. *Water (Switzerland)*, *12*(5). https://doi.org/10.3390/W12051374

Georgieva, V. G., Gonsalvesh, L., & Tavlieva, M. P. (2020). Thermodynamics and kinetics of the removal of nickel (II) ions from aqueous solutions by biochar adsorbent made from agro-waste walnut shells. *Journal of Molecular Liquids*, *312*. https://doi.org/10.1016/j.molliq.2020.112788

Gerard, A. Y., Kautz, E. J., Schreiber, D. K., Han, J., McDonnell, S., Ogle, K., Lu, P., Saal, J. E., Frankel, G. S., & Scully, J. R. (2023). The role of chromium content in aqueous passivation of a non-equiatomic Ni38Fe20CrxMn21-0.5xCo21-0.5x multi-principal element alloy (x = 22, 14, 10, 6 at%) in acidic chloride solution. *Acta Materialia*, *245*. https://doi.org/10.1016/j.actamat.2022.118607

Gkika, D. A., Mitropoulos, A. C., & Kyzas, G. Z. (2022). Why reuse spent adsorbents? The latest challenges and limitations. In *Science of the Total Environment* (Vol. 822). Elsevier B.V. https://doi.org/10.1016/j.scitotenv.2022.153612

GracePavithra, K., Jaikumar, V., Kumar, P. S., & SundarRajan, P. S. (2019). A review on cleaner strategies for chromium industrial wastewater: Present research and future perspective. In *Journal of Cleaner Production* (Vol. 228, pp. 580–593). Elsevier Ltd. https://doi.org/10.1016/j.jclepro.2019.04.117

Guo, Y., Gong, Z., Li, C., Gao, B., Li, P., Wang, X., Zhang, B., & Li, X. (2020). Efficient removal of uranium (VI) by 3D hierarchical Mg/Fe-LDH supported nanoscale hydroxyapatite: A synthetic experimental and mechanism studies. *Chemical Engineering Journal*, *392*. https://doi.org/10.1016/j.cej.2019.123682

Hasan, M. B., Al-Tameemi, I. M., & Abbas, M. N. (2021). Orange Peels as a Sustainable Material for Treating Water Polluted with Antimony. *Journal of Ecological Engineering*, *22*(2), 25–35. https://doi.org/10.12911/22998993/130632

Hayashi, N., Matsumura, D., Hoshina, H., Ueki, Y., Tsuji, T., Chen, J., & Seko, N. (2021). Chromium(VI) adsorption–reduction using a fibrous amidoxime-grafted adsorbent. *Separation and Purification Technology*, *277*. https://doi.org/10.1016/j.seppur.2021.119536

Inam, M. A., Khan, R., Inam, M. W., & Yeom, I. T. (2021). Kinetic and isothermal sorption of antimony oxyanions onto iron hydroxide during water treatment by coagulation process. *Journal of Water Process Engineering*, *41*. https://doi.org/10.1016/j.jwpe.2021.102050

Inam, M. A., Khan, R., Park, D. R., Khan, S., Uddin, A., & Yeom, I. T. (2019). Complexation of antimony with natural organic matter: Performance evaluation during coagulation-flocculation process. *International Journal of Environmental Research and Public Health*, *16*(7). https://doi.org/10.3390/ijerph16071092

Inam, M. A., Khan, R., Park, D. R., Lee, Y. W., & Yeom, I. T. (2018). Removal of Sb(III) and Sb(V) by ferric chloride coagulation: Implications of Fe solubility. *Water (Switzerland)*, *10*(4). https://doi.org/10.3390/w10040418

Irem, S., Islam, E., Mahmood Khan, Q., Ul Haq, M. A., & Jamal Hashmat, A. (2017). Adsorption of arsenic from drinking water using natural orange waste: Kinetics and fluidized bed column studies. *Water Science and Technology: Water Supply*, *17*(4), 1149–1159. https://doi.org/10.2166/ws.2017.009

JishaTJ, LubnaCH, & HabeebaV. (2017). *REMOVAL OF Cr (VI) USING ORANGE PEEL AS AN ADSORBENT* (Vol. 3). www.ijariie.com

Jnr, M. H., & Spiff, A. I. (2005). Effects of temperature on the sorption of Pb 2+ and Cd 2+ from aqueous solution by Caladium bicolor (Wild Cocoyam) biomass. In *Electronic Journal of Biotechnology* (Vol. 8, Issue 2). http://www.ejbiotechnology.info/content/vol8/issue2/full/4/

Kajama, M. N. (2015). Hydrogen permeation using nanostructured silica membranes. *Sustainable Development and Planning VII*, *1*, 447–456. https://doi.org/10.2495/sdp150381

Kane, S. N., Mishra, A., & Dutta, A. K. (2016). Preface: International Conference on Recent Trends in Physics (ICRTP 2016). In *Journal of Physics: Conference Series* (Vol. 755, Issue 1). Institute of Physics Publishing. https://doi.org/10.1088/1742-6596/755/1/011001

Kang, D., Yu, X., Tong, S., Ge, M., Zuo, J., Cao, C., & Song, W. (2013). Performance and mechanism of Mg/Fe layered double hydroxides for fluoride and arsenate removal from aqueous solution. *Chemical Engineering Journal*, *228*, 731–740. https://doi.org/10.1016/j.cej.2013.05.041

Karimi-Maleh, H., Ayati, A., Ghanbari, S., Orooji, Y., Tanhaei, B., Karimi, F., Alizadeh, M., Rouhi, J., Fu, L., & Sillanpää, M. (2021). Recent advances in removal techniques of Cr(VI) toxic ion from aqueous solution: A comprehensive review. In *Journal of Molecular Liquids* (Vol. 329). Elsevier B.V. https://doi.org/10.1016/j.molliq.2020.115062

Kocaoba, S., Cetin, G., & Akcin, G. (2022). Chromium removal from tannery wastewaters with a strong cation exchange resin and species analysis of chromium by MINEQL+. *Scientific Reports*, *12*(1). https://doi.org/10.1038/s41598-022-14423-3

Korus, I., & Loska, K. (2009). Removal of Cr(III) and Cr(VI) ions from aqueous solutions by means of polyelectrolyte-enhanced ultrafiltration. *Desalination*, *247*(1–3), 390–395. https://doi.org/10.1016/j.desal.2008.12.036

Kumar, A., & Jena, H. M. (2017). Adsorption of Cr(VI) from aqueous phase by high surface area activated carbon prepared by chemical activation with ZnCl2. *Process Safety and Environmental Protection*, *109*, 63–71. https://doi.org/10.1016/j.psep.2017.03.032

Kuppusamy, P., Yusoff, M. M., Maniam, G. P., & Govindan, N. (2016). Biosynthesis of metallic nanoparticles using plant derivatives and their new avenues in pharmacological applications

– An updated report. In *Saudi Pharmaceutical Journal* (Vol. 24, Issue 4, pp. 473–484). Elsevier B.V. https://doi.org/10.1016/j.jsps.2014.11.013

Li, G. J., Yang, C., Yao, Y., & Zeng, M. (2019). Electrocoagulation of chromium in tannery wastewater by a composite anode modified with titanium: Parametric and kinetic study. *Desalination and Water Treatment*, *171*, 294–301. https://doi.org/10.5004/dwt.2019.24792

Li, H., Dong, X., da Silva, E. B., de Oliveira, L. M., Chen, Y., & Ma, L. Q. (2017). Mechanisms of metal sorption by biochars: Biochar characteristics and modifications. In *Chemosphere* (Vol. 178, pp. 466–478). Elsevier Ltd. https://doi.org/10.1016/j.chemosphere.2017.03.072

Li, Z., Fang, X., Yuan, W., Zhang, X., Yu, J., Chen, J., & Qiu, X. (2023). Preparing of layered double hydroxide- alginate microspheres for Cr(VI)-contaminated soil remediation. *Colloids and Surfaces A: Physicochemical and Engineering Aspects*, *658*. https://doi.org/10.1016/j.colsurfa.2022.130655

Maamoun, I., Bensaida, K., Eljamal, R., Falyouna, O., Tanaka, K., Tosco, T., Sugihara, Y., & Eljamal, O. (2022). Rapid and efficient chromium (VI) removal from aqueous solutions using nickel hydroxide nanoplates (nNiHs). *Journal of Molecular Liquids*, *358*. https://doi.org/10.1016/j.molliq.2022.119216

Maamoun, I., Falyouna, O., Eljamal, R., Bensaida, K., Tanaka, K., Tosco, T., Sugihara, Y., & Eljamal, O. (2022). Multi-functional magnesium hydroxide coating for iron nanoparticles towards prolonged reactivity in Cr(VI) removal from aqueous solutions. *Journal of Environmental Chemical Engineering*, *10*(3). https://doi.org/10.1016/j.jece.2022.107431

MacAdams, L. A., Buffone, G. P., Incarvito, C. D., Rheingold, A. L., & Theopold, K. H. (2005). A chromium catalyst for the polymerization of ethylene as a homogeneous model for the Phillips catalyst. *Journal of the American Chemical Society*, *127*(4), 1082–1083. https://doi.org/10.1021/ja043877x

Madhuranthakam, C. M. R., Thomas, A., Akhter, Z., Fernandes, S. Q., & Elkamel, A. (2021). Removal of Chromium(VI) from Contaminated Water Using Untreated Moringa Leaves as Biosorbent. *Pollutants*, *1*(1), 51–64. https://doi.org/10.3390/pollutants1010005

Meili, L., Lins, P. V., Zanta, C. L. P. S., Soletti, J. I., Ribeiro, L. M. O., Dornelas, C. B., Silva, T. L., & Vieira, M. G. A. (2019). MgAl-LDH/Biochar composites for methylene blue removal by adsorption. *Applied Clay Science*, *168*, 11–20. https://doi.org/10.1016/j.clay.2018.10.012

Mekonnen, D. T., Alemayehu, E., & Lennartz, B. (2021). Fixed-bed column technique for the removal of phosphate from water using leftover coal. *Materials*, *14*(19). https://doi.org/10.3390/ma14195466

Miretzky, P., & Cirelli, A. F. (2010). Cr(VI) and Cr(III) removal from aqueous solution by raw and modified lignocellulosic materials: A review. In *Journal of Hazardous Materials* (Vol. 180, Issues 1–3, pp. 1–19). https://doi.org/10.1016/j.jhazmat.2010.04.060

Moges, A., Nkambule, T. T. I., & Fito, J. (2022). The application of GO-Fe3O4 nanocomposite for chromium adsorption from tannery industry wastewater. *Journal of Environmental Management*, *305*. https://doi.org/10.1016/j.jenvman.2021.114369

Mondal, S. K., & Saha, P. (2018). Separation of hexavalent chromium from industrial effluent through liquid membrane using environmentally benign solvent: A study of experimental optimization through response surface methodology. *Chemical Engineering Research and Design*, *132*, 564–583. https://doi.org/10.1016/j.cherd.2018.02.001

Mustapha, S., Shuaib, D. T., Ndamitso, M. M., Etsuyankpa, M. B., Sumaila, A., Mohammed, U. M., & Nasirudeen, M. B. (2019). Adsorption isotherm, kinetic and thermodynamic studies for the removal of Pb(II), Cd(II), Zn(II) and Cu(II) ions from aqueous solutions using Albizia lebbeck pods. *Applied Water Science*, *9*(6). https://doi.org/10.1007/s13201-019-1021-x

Mutongo, F., Kuipa, O., & Kuipa, P. K. (2014). Removal of Cr(VI) from aqueous solutions using powder of potato peelings as a low cost sorbent. *Bioinorganic Chemistry and Applications*, *2014*. https://doi.org/10.1155/2014/973153

Nejati, K., Asadpour-Zeynali, K., Rezvani, Z., & Peyghami, R. (2014). Determination of 2-Nitrophenol by Electrochemical Synthesized Mg/Fe Layered Double Hydroxide Sensor. In *Int. J. Electrochem. Sci* (Vol. 9). www.electrochemsci.org

Omitola, O. B., Abonyi, M. N., Akpomie, K. G., & Dawodu, F. A. (2022). Adams-Bohart, Yoon-Nelson, and Thomas modeling of the fix-bed continuous column adsorption of amoxicillin onto silver nanoparticle-maize leaf composite. *Applied Water Science*, *12*(5). https://doi.org/10.1007/s13201-022-01624-4

Özer, D., Aksu, Z., Kutsal, T., & Çaglar, A. (1994). Adsorption isotherms of lead(ii) and chromium(vi) on cladophora crispata. *Environmental Technology (United Kingdom)*, *15*(5), 439–448. https://doi.org/10.1080/09593339409385448

Padmavathy, K. S., Madhu, G., & Haseena, P. V. (2016). A study on Effects of pH, Adsorbent Dosage, Time, Initial Concentration and Adsorption Isotherm Study for the Removal of Hexavalent Chromium (Cr (VI)) from Wastewater by Magnetite Nanoparticles. *Procedia Technology*, *24*, 585–594. https://doi.org/10.1016/j.protcy.2016.05.127

Park, J. E., Shin, J. H., Oh, W., Choi, S. J., Kim, J., Kim, C., & Jeon, J. (2022). Removal of Hexavalent Chromium(VI) from Wastewater Using Chitosan-Coated Iron Oxide Nanocomposite Membranes. *Toxics*, *10*(2). https://doi.org/10.3390/toxics10020098

Peng, H., Leng, Y., & Guo, J. (2019). Electrochemical removal of chromium (VI) from wastewater. *Applied Sciences (Switzerland)*, *9*(6). https://doi.org/10.3390/app9061156

Peng, Y., Xiao, H. Y., Cheng, X. Z., & Chen, H. M. (2013). Removal of arsenic from wastewater by using pretreating orange peel. *Advanced Materials Research*, *773*, 889–892. https://doi.org/10.4028/www.scientific.net/AMR.773.889

Pertile, E., Dvorský, T., Václavík, V., & Heviánková, S. (2021). Use of different types of biosorbents to remove cr (Vi) from aqueous solution. *Life*, *11*(3). https://doi.org/10.3390/life11030240

Prajapati, A. K., Das, S., & Mondal, M. K. (2020). Exhaustive studies on toxic Cr(VI) removal mechanism from aqueous solution using activated carbon of Aloe vera waste leaves. *Journal of Molecular Liquids*, *307*. https://doi.org/10.1016/j.molliq.2020.112956

Puccini, M., Licursi, D., Stefanelli, E., Vitolo, S., Galletti, A. M. R., & Heeres, H. J. (2016). Levulinic acid from orange peel waste by hydrothermal carbonization (HTC). *Chemical Engineering Transactions*, *50*, 223–228. https://doi.org/10.3303/CET1650038

Rai, M. K., Shahi, G., Meena, V., Meena, R., Chakraborty, S., Singh, R. S., & Rai, B. N. (2016). Removal of hexavalent chromium Cr (VI) using activated carbon prepared from mango kernel activated with H3PO4. *Resource-Efficient Technologies*, *2*, S63–S70. https://doi.org/10.1016/j.reffit.2016.11.011

Rattanarat, P., Dungchai, W., Cate, D. M., Siangproh, W., Volckens, J., Chailapakul, O., & Henry, C. S. (2013). A microfluidic paper-based analytical device for rapid quantification of particulate chromium. *Analytica Chimica Acta*, *800*, 50–55. https://doi.org/10.1016/j.aca.2013.09.008

Revellame, E. D., Fortela, D. L., Sharp, W., Hernandez, R., & Zappi, M. E. (2020). Adsorption kinetic modeling using pseudo-first order and pseudo-second order rate laws: A review. In *Cleaner Engineering and Technology* (Vol. 1). Elsevier Ltd. https://doi.org/10.1016/j.clet.2020.100032

S. Adachi. (1987). *EFFECTS OF CHROMIUM COMPOUNDS ON THE RESPIRATORY SYSTEM Part 5. Long Term Inhalation of Chromic Acid Mist in Electroplating by C57BL Female Mice and Recapitulation on Our Experimental Studies Shuichi ADACHI*.*

Saha, B., Amine, A., & Verpoort, F. (2022). Special Issue: Hexavalent Chromium: Sources, Toxicity, and Remediation. In *Chemistry Africa* (Vol. 5, Issue 6, pp. 1779–1780). Springer Science and Business Media Deutschland GmbH. https://doi.org/10.1007/s42250-022-00443-z

Santos, L. C., da Silva, A. F., dos Santos Lins, P. V., da Silva Duarte, J. L., Ide, A. H., & Meili, L. (2020). Mg-Fe layered double hydroxide with chloride intercalated: synthesis, characterization and application for efficient nitrate removal. *Environmental Science and Pollution Research*, *27*(6), 5890–5900. https://doi.org/10.1007/s11356-019-07364-4

Shakya, A., Núñez-Delgado, A., & Agarwal, T. (2019). Biochar synthesis from sweet lime peel for hexavalent chromium remediation from aqueous solution. *Journal of Environmental Management*, *251*. https://doi.org/10.1016/j.jenvman.2019.109570

Sharma, P., Singh, S. P., Parakh, S. K., & Tong, Y. W. (2022). Health hazards of hexavalent chromium (Cr (VI)) and its microbial reduction. In *Bioengineered* (Vol. 13, Issue 3, pp. 4923–4938). Taylor and Francis Ltd. https://doi.org/10.1080/21655979.2022.2037273

Sreeram, K. J., & Ramasami, T. (2003). *Sustaining tanning process through conservation, recovery and better utilization of chromium*. www.elsevier.com/locate/resconrec

Verger, L., Dargaud, O., Chassé, M., Trcera, N., Rousse, G., & Cormier, L. (2018). Synthesis, properties and uses of chromium-based pigments from the Manufacture de Sèvres. *Journal of Cultural Heritage*, *30*, 26–33. https://doi.org/10.1016/j.culher.2017.09.012

Wahid, F., Shah, A. U., Rahim, M., Dad, F., Khan, N., Ullah, S., Ali, Y., & Shah, S. A. A. (2021). Contamination Level of Chromium, Iron, Nickel, Lead and Cobalt in Soil from an Agricultural area of Urmar Bala, Peshawar Pakistan. *Journal of Innovative Sciences*, *7*(1). https://doi.org/10.17582/journal.jis/2021/7.1.161.166

Wang, Y., Su, H., Gu, Y., Song, X., & Zhao, J. (2017). Carcinogenicity of chromium and chemoprevention: A brief update. In *OncoTargets and Therapy* (Vol. 10, pp. 4065–4079). Dove Medical Press Ltd. https://doi.org/10.2147/OTT.S139262

Xu, D., Zhou, B., & Yuan, R. (2019). Optimization of coagulation-flocculation treatment of wastewater containing Zn(II) and Cr(VI). *IOP Conference Series: Earth and Environmental Science*, *227*(5). https://doi.org/10.1088/1755-1315/227/5/052049

Xu, T., Zhou, Y., Lei, X., Hu, B., Chen, H., & Yu, G. (2019). Study on highly efficient Cr(VI) removal from wastewater by sinusoidal alternating current coagulation. *Journal of Environmental Management*, *249*. https://doi.org/10.1016/j.jenvman.2019.109322

Xue, L., Gao, B., Wan, Y., Fang, J., Wang, S., Li, Y., Muñoz-Carpena, R., & Yang, L. (2016). High efficiency and selectivity of MgFe-LDH modified wheat-straw biochar in the removal of nitrate from aqueous solutions. *Journal of the Taiwan Institute of Chemical Engineers*, *63*, 312–317. https://doi.org/10.1016/j.jtice.2016.03.021

Yu, Y., Shironita, S., Souma, K., & Umeda, M. (2018). *Effect of chromium content on the corrosion resistance of ferritic stainless steels in sulfuric acid solution*. https://doi.org/10.1016/j.heliyon.2018

Zhang, L., Huang, Z., Chang, L., & Zheng, Q. (2017). Comparison of oxidation behaviors of Cr7C3 at 1173 K and 1273 K. *Materials Research Express*, *4*(10). https://doi.org/10.1088/2053-1591/aa8d36

Zhou, T., Fang, L., Wang, X., Han, M., Zhang, S., & Han, R. (2017). Adsorption of the herbicide 2,4-dichlorophenoxyacetic acid by Fe-crosslinked chitosan complex in batch mode. *Desalination and Water Treatment*, *70*, 294–301. https://doi.org/10.5004/dwt.2017.20508

Zolfaghari, G., & Kargar, M. (2019). Nanofiltration and microfiltration for the removal of chromium, total dissolved solids, and sulfate from water. *MethodsX*, *6*, 549–557. https://doi.org/10.1016/j.mex.2019.03.012

MS Thesis

ORIGINALITY REPORT

2%	2%	2%	0%
SIMILARITY INDEX	INTERNET SOURCES	PUBLICATIONS	STUDENT PAPERS

PRIMARY SOURCES

1	Muhammad Ali Inam, Rizwan Khan, Muhammad Waleed Inam, Ick Tae Yeom. "Kinetic and isothermal sorption of antimony oxyanions onto iron hydroxide during water treatment by coagulation process", Journal of Water Process Engineering, 2021 Publication	1%
2	gyan.iitg.ernet.in Internet Source	1%
3	opus.lib.uts.edu.au Internet Source	1%

Exclude quotes	Off	Exclude matches	< 1%
Exclude bibliography	On		